EÖTVÖS LORÁND UNIVERSITY

FACULTY OF INFORMATICS

DEPARTMENT OF CARTOGRAPHY AND GEOINFORMATICS

# Case Study: Scenarios of Northern Nile Delta Submergence using SRTM and GEBCO Bathymetry

**Ahmed Hamido**

Senior student of Cartography MSc.

**András Jung**

Associate Professor

ELTE Department of Cartography and Geoinformatics

Budapest, 2023

# ACKNOWLEDGEMENT

I would truly like to thank my supervisor, Dr. Jung András for his unwavering support and guidance throughout my master's thesis journey. His patience, encouragement, and expertise have been instrumental not only in helping me achieve my academic goals, but also for gaining my summer internship at GFZ. I appreciate his generosity in giving his time and attention to my project. Sincere thanks from the bottom of my heart goes to Dr. Islam Hamdy as I am indebted to him for his time and relentless effort, he invested with me throughout the project. His usual availability for online meetings, hints, and modifications he kept highlighting made the best out of this research.

Also, I would like to extend my sincere thanks to Prof. Hamdy El-Gamily, CEO of GIG company in Egypt and minister's advisor for GIS for sharing his welcoming attitude, knowledge, time and expertise from the very beginning, along with Dr. Mohamed Elrawy for sharing his videos and lectures about hydrology and water analysis. Thanks once more to ELTE and all the professors who taught me a lot at the Institute of Cartography and Geoinformatics. I also thank the Stipendium Hungaricum scholarship and the Cultural Affairs and Missions Sector in Egypt for giving me the opportunity to pursue another degree after my bachelor’s here in such a magnificent country like Hungary.  Finally, I will always be thankful to my partner Bianka who supported me since I arrived in Hungary as well as my parents who have consistently supported me unfailingly during my whole life and pushed me towards pursuing a master’s degree.

# Table of Contents

# List of Abbreviations

| | |
|---|---|
| **AOI** | Area of Interest |
| **ASTER** | Advanced Spaceborne Thermal Emission and Reflection Radiometer |
| **BODC** | British Oceanographic Data Centre |
| **CAPMAS** | Central Agency for Public Mobilization and Statistics |
| **DEM** | Digital Elevation Model |
| **DSM** | Digital Surface Model |
| **GDEM** | Global Digital Elevation Model |
| **GIA** | Glacier Isostatic Adjustment |
| **GIS** | Geographic Information System |
| **GEBCO** | General Bathymetric Chart of the Oceans |
| **GMSL** | Global Mean Sea Level |
| **GNSS** | Global navigation satellite system |
| **GPS** | Global Positioning System |
| **IFPRI** | International Food Policy Research Institute |
| **IHO** | International Hydrographic Organization |
| **InSAR** | Interferometric Synthetic Aperture Radar |
| **IPCC** | Intergovernmental Panel on Climate Change |
| **LIDAR** | Light Detection and Ranging |
| **NAO** | North Atlantic Oscillation |
| **NASA** | National Aeronautics and Space Administration |
| **NGA** | National Geospatial-Intelligence Agency |
| **PDO** | Pacific Decadal Oscillation |
| **RMSE** | Root Mean Square Error |
| **SAR** | Synthetic Aperture Radar |
| **SDGs** | Sustainable Development Goals |
| **SIR-C-SAR** | Spaceborne Imaging Radar-C band Synthetic Aperture Radar |
| **SLR** | Sea Level Rise |
| **SRTM** | Shuttle Radar Topography Mission |
| **TID** | Type Identifier |

## List of Figures

## List of Tables

# ABSTRACT

Future Sea Level Rise (SLR) poses a significant threat to the deltas around the world including the Nile Delta. Land subsidence and human-induced land degradation are amongst the top challenges that the region is facing which can exacerbate the impact of SLR. Potential threats such as coastal flooding, erosion, and saltwater intrusion into freshwater resources could have impactful socio-economic and environmental consequences in the region. Therefore, there is an urge to use remote sensing and Geographic Information System (GIS) techniques to create comprehensive vulnerability and risk assessments. This thesis work simulates different SLR scenarios ranging from 1 to 4 meters in the northern delta region, which is highly vulnerable due to its low-lying topography and high population density. Shuttle Radar Topography Mission (SRTM1) and the General Bathymetric Chart of the Oceans (GEBCO) were utilized to conduct the geospatial analysis, and the results were compared eventually. GEBCO proved to be suitable for such a small-scale area despite its lower resolution (~450 m) as its processing was faster and its results aligned with SRTM results which have relatively higher spatial resolution (30 m).

The results indicate that Port Said, Damietta and Kafr El-Sheikh will suffer severely from 2 m SLR that could be reached by 2100 by losing more than half of their areas and 4 m SLR will have catastrophic effect on most of the governorates in the region such as Alexandria that will lose one-fourth of its total area. Overall, the study provides valuable insights into potential impacts of SLR on the northern Nile Delta and highlights the importance of accurate DEMs for managing and monitoring the coastal environments. It also reveals that different adaptation methods like land use regulations, coastal protection structures, and sustainable water management are key factors in mitigating the potential impacts in the region.

Keywords: DEM, GEBCO, Land use, Nile delta, SLR, SRTM

# 1. INTRODUCTION

Climate change and global warming have taken part significantly in raising the global sea levels recently worldwide. The effects of global warming can cause serious threats to the surrounding environment, human welfare and socio-economic activities. Sea level rise (SLR) can be caused by global warming via expanding the ocean water, melting mountainous glaciers, and eventually causing polar glaciers to melt and slip into the oceans. Since 1880, the global mean sea level (GMSL) has risen around 21-24 centimeters and in 2021, 97 millimeters of GMSL was recorded above 1993 levels (Lindsey, 2022). That made it the highest annual average to be in the satellite record (1993-present). Across most of the world's oceans (blue colors), mean sea level has risen between 1993 and 2021 as shown below (**Figure** 1).

According to Reuters, around 1.47 billion people globally today are at the risk of intense flooding. When it comes to Egypt, the sea level has been rising by 3.2 mm since 2012 annually, which threatens to erode and flood the Nile Delta’s northern shore. This means pushing saltwater further into the soil and groundwater that farmers use for irrigation. Based on the data from the University of East Anglia's Climatic Research Unit, temperatures in Egypt have increased by 0.4 degrees Celsius per decade over the past 30 years. Far apart from SLR and according to a paper by the International Food Policy Research Institute (IFPRI), yields for food crops in Egypt are expected to drop by more than 10% by 2050 due to increased salinity of irrigation water, higher temperatures and water stress.

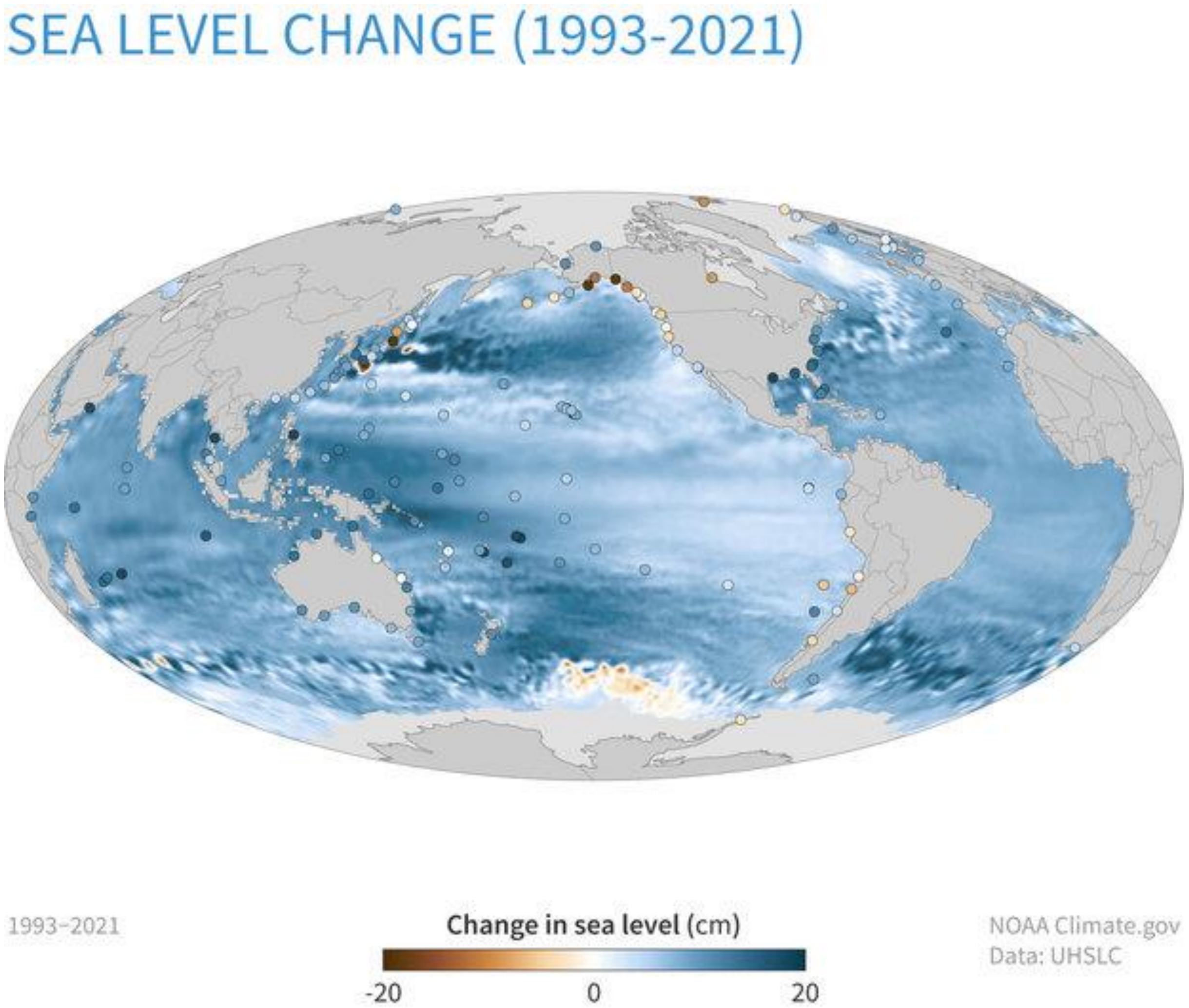


***Figure 1.*** *A map showing mean sea level rise across most of the world's oceans (Blue colors) and rates of local sea level (dots) that can be larger than the global average. (NOAA Climate.gov based on data provided by Philip Thompson, University of Hawaii)*

Egyptians dwelled in the Nile Delta thousands of years ago where the cradle of civilization of ancient Egypt started. They have successfully coped with the positive and negative effects such as floods that brought a lot of sediments and alluvium to the area. In 1780, people started to interact with both the Nile and Delta. For instance, seawalls (**Figure** 2) were amongst the first protective barriers like Mohamed Ali Sea Wall in Abu Quir Bay, Alexandria (Haars et al., 2016). Recently in the 20th century, the human impact on the natural system has been severe and still ongoing. Major dams were constructed to store the excessive Nile water like the High Dam in Aswan. Coastal dune lands and wetlands transformed into urban areas as well as agricultural and aquacultural lands.

***Figure 2.*** *An image showing the weakness of erected seawalls on Alexandria shore. (Eldeberky, 2011)*

### 1.1. Nile Delta Description

The Nile Delta is formed in Lower Egypt where we can see after passing Cairo, the capital of Egypt, the Nile River divides into 2 branches: Damietta in the east and Rosetta in the west (**Figure** 3). It is relatively flat and encompasses 25% of the total Mediterranean coastal wetlands as it occupies approximately 20,000 km$^2$ and represents 2.3% of the whole country's area. The Delta's shoreline extends 275 km, and it contributes to the agricultural production with 30-40% and 60% of the fish catchment in the marine environments (Abou Samra et al., 2021). It is well-known that the Nile Delta is one of the largest river deltas in the world. It is worth mentioning that around 90% of the population lives along Egypt's Nile basin and 50% live in the Delta itself, this roughly represents 40 million people with a population density outside the major cities of average 1000/km$^2$ or more (Haars et al., 2016).

The Nile Delta in Egypt belongs to the coastal landforms that are most vulnerable to inundation and SLR is expected to threaten its coastal zone, agricultural productivity, water resources and population (Elshinnawy & Almaliki, 2021). The Nile River has always been the lifeline for Egypt and the Egyptians as it provided the Delta soil which contains mineral supplies and natural nutrients that enriches the fertile soil and made the Delta such an important agricultural region. Three large brackish lakes occupy the Delta's shoreline which are: Idku, Burullus and Manzala (Hasan et al., 2015).

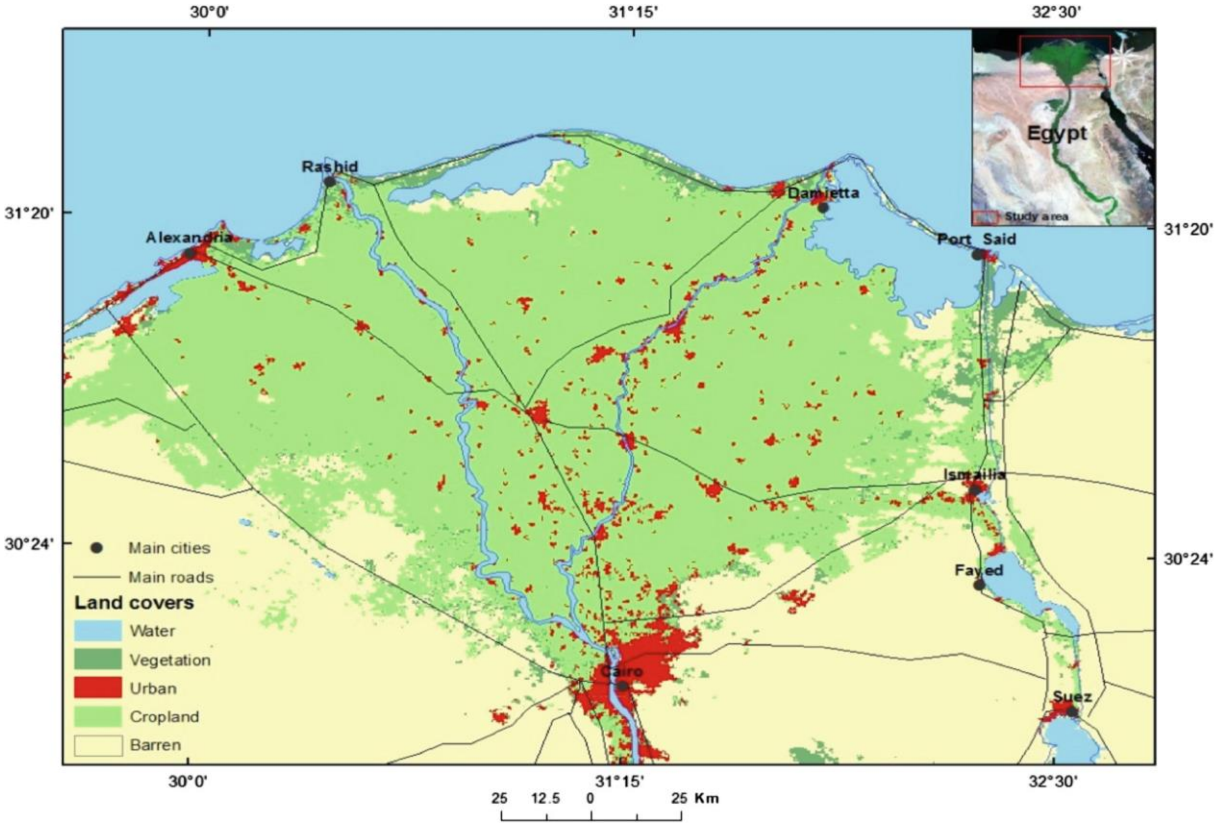


*__Figure 3.__ A map of the Nile Delta, Egypt showing the 3 main lakes occupying the shoreline, main cities and land cover types from MODIS data. (Hasan et al., 2015)*

## 1.2. Aim of Research

In this research, we aim to investigate the area of the northern Nile Delta using the Shuttle Radar Topography Mission (SRTM) Digital Elevation Model (DEM) and the General Bathymetric Chart of the Oceans (GEBCO). The northern part of the Delta comprises the major cities that are at the risk of inundation by SLR which are: Alexandria, Gharbia, Kafr El-Sheikh, Dakahlia, Damietta and Port Said. These geodetic remote sensing techniques using Spaceborne Imaging Radar-C band Synthetic Aperture Radar (SIR-C-SAR) for SRTM and multi-beam echo data from GECBO provide us with a high-resolution digital topographic database. With processing the DEMs and performing raster calculations for different SLR scenarios, we can make risk assessment and monitor the coastal zones that are vulnerable to inundation due to SLR.

Our secondary aim is to check the reliability and accuracy of these 2 different techniques and compare the resulting inundated areas, specially that they both can be freely accessed and up to date. Recently, there is a global call for geo-conservation and protecting our infrastructure and artifacts urged by the UN and UNESCO. The 13th goal of the sustainable development goals (SDGs) is to take an urgent action to combat climate change and its impacts. Such areas like the Nile Delta and other low-lying lands usually concentrate high exposure of population and economic activity to the impacts of climate hazards. Therefore, it is recommended and crucial to keep monitoring the regions and coastal zones that are under changing scenarios of global climate change and SLR and come up with planned adaptation strategies.

### 1.3. SLR History and its Impacts on The Nile Delta

Since the end of the 19th century, the SLR has been a prominent phenomenon that started to draw a lot of scientists' attention. In the past 100 years, sea level changes observations have been made in two ways; one is using radar altimeters installed in satellites and the other is tide gauge observation. It is not an easy task to estimate the GMSL directly, because uniform and dense observations are needed for entire oceans (Mimura, 2013). Satellite altimetry has become the main technique used for measuring the sea level precisely and continuously since the early 1990s. This is because of its advantages over tide gauges such as its regular global coverage with frequent revisit time and lack of influence of land movement.

Similar Studies were conducted (Church & White, 2011) to summarize the contemporary GMSL. In the figure below (**Figure** 4), it shows a summary of the long-term trend from 1860-2010 of GMSL resulting from superposing the 2 sources of observed data. We can see in that graph the rate of increase in GMSL was not large until 1930, but it has increased at an accelerating rate since then. It was indicated (Church & White, 2011) that the increase in GMSL from 1880 to 2009 was 21 cm and this rate of increment doubled to 3.2 ± 0.4 mm/year for 1993-2009 relative to 1900-2009 when it was 1.7 ± 0.2 mm/year.

The change of GMSL for 1993 to 2009 obtained by satellite altimeters is represented in **Figure** 5 (Cazenave & Llovel, 2010), which corresponds to the latter part of **Figure** 4. A sudden increase in GMSL was indicated from 1997 to 1999, and a decrease in 2008. These uncommon changes are considered to be from an intense El Niño during 1997 to 1998, and La Niña in 2007. They also identified the influence of Pacific Decadal Oscillation (PDO) and North Atlantic Oscillation (NAO) leading to long-term fluctuations with a period of 10-20 years.

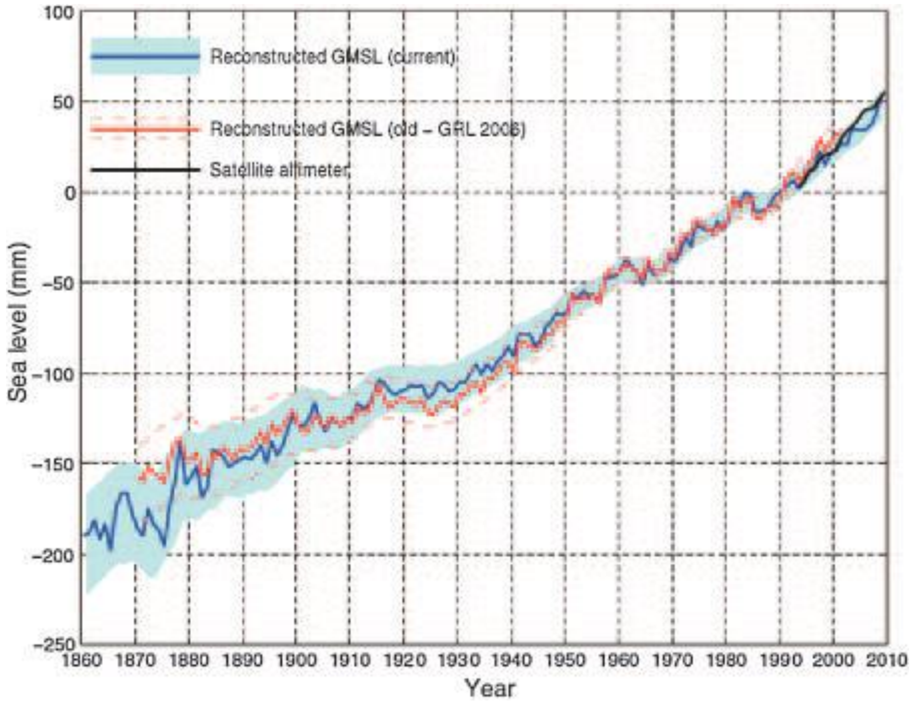


***Figure 4.*** *A graph for GMSL from 1860 to 2009. Blue line: estimated from coastal and island sea-level data with one standard deviation error (shading), Red line: estimated by Church and White (2006) for 1870–2001 (solid line) with one standard deviation error (dashed lines). Black line: satellite altimeter data since 1993. (Church & White, 2006; Church & White, 2011)*

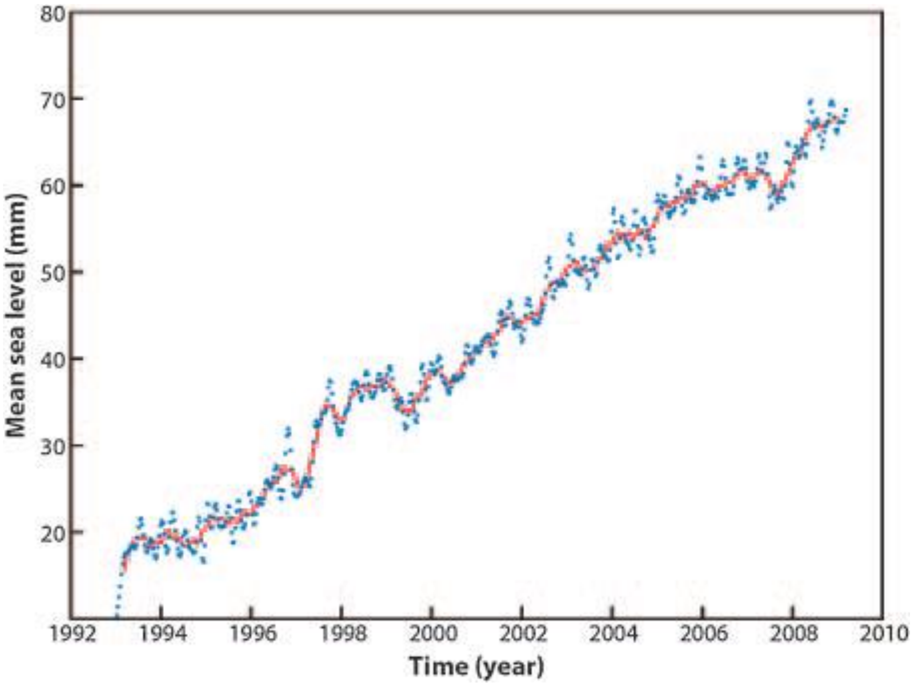


***Figure 5.*** *A graph showing GMSL from satellite altimetry for 1993 to 2008. Blue dots are raw 10-day data, where the red line corresponds to a 90-day smoothing of the raw data. The -0.3mm/year Glacial Isostatic Adjustment (GIA) correction was applied. (Cazenave & Llovel, 2010)*

Multiple factors can cause changes in SLR, mostly the change in total volume of sea water and movements of ocean bottom and ground that directly affect the shape and size of the ocean basins. Also, some dynamic factors play a key role in this process such as atmospheric pressure, wind, ocean currents and waves. Therefore, many factors with various spatial and temporal scale are directly related to sea water volume changes in ocean basins as shown below (Cazenave & Llovel, 2010; Mimura, 2013):

1) Factors accompanying changes in sea water volume in ocean basins
    - Thermal expansion of sea water
    - Growth/decay of ice sheets, e.g., Greenland Ice Sheet & West Antarctica Ice Sheet
    - Terrestrial water storage, such as lakes, dam reservoirs and groundwater depletion

2) Factors accompanying changes in the shape and size of ocean basins
    - Isostatic adjustment of land masses, especially Glacial Isostatic Adjustment (GIA)
    - Tectonic movements including ground subsidence or uplift related to earthquakes
    - Ground subsidence or uplift due to ground compaction and groundwater pumping
    - Sediment inflow from the lands

3) Other factors causing local or temporal changes in sea level
   - Changes in ocean current and atmospheric pressure
   - Tides, Tsunamis, waves and storm surges
   - Inter-annual natural variations, such as PDO

An earlier estimation was made by The Intergovernmental Panel of Climate Change (IPCC) stating that the global mean seawater levels have risen by 10-20 cm in the last century and during this century, it will reach the range of 11-88 cm (IPCC, 2001). According to Sefelnasr and Sherif (2013), the increase in seawater levels due to climate change can lead to severe impacts in coastal aquifers. First, there will be a shift for the shoreline to a new landward position and this shift may be significant depending on the land topography and the groundwater in the area will become totally saline. Second, it will cause more extra pressure at the seaside and hence, the water will advance more inland. Third, variations in rainfall may happen by climate change which will affect the replenishment of the groundwater. Finally, reliance on exploration of groundwater resources will increase to substitute for surface water resources scarcity and meet the demands of different sectors due to anticipated reduction in waterfall and water resources in arid and semi-arid areas.

Sea levels were 100 m lower than today 15,000-20,000 years ago. Due to the above-mentioned causes, there was a rapid rise in the sea level about 8 mm/year, however, the rates then decreased which allowed the delta to form (Frihy, 2003). In the next 50-100 years, it is predicted that there would be an increase of 50-150 cm. One of the factors that were discussed earlier is land subsidence and the Nile Delta has been going through it recently. Its average subsidence is about 5 mm/year ranging from 0.5-7 mm/year as mentioned by Stanley (1990) and shown in **Figure** 6 below.

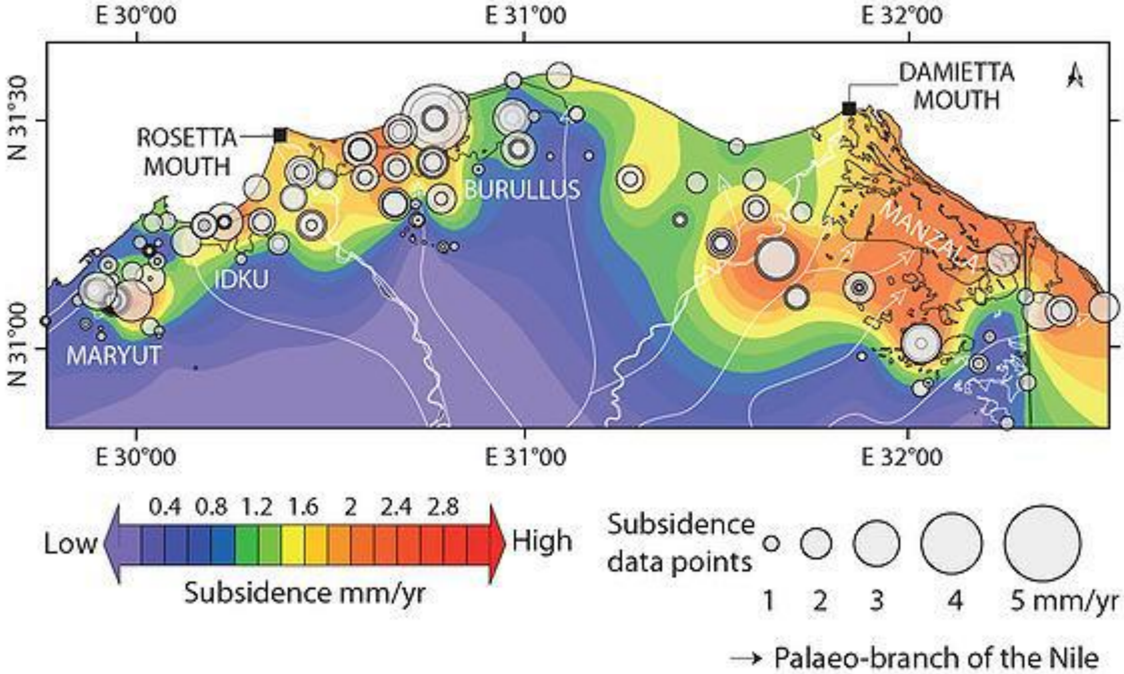


***Figure 6.*** *A map showing the annual subsidence in the northern Nile Delta. (Marriner et al., 2012).*

Tectonic movements on the fault lines of the deeply buried strata or excessive groundwater extraction could be the main causes for subsidence in the delta. As a consequence of the future SLR in the Nile Delta, there will be more coastal erosion, inundation of wetlands and saltwater intrusion into the Nile River and groundwater (El Nahry & Doluschitz, 2010; El-Quilish et al., 2022). As it is shown below **Figure** 7, major cities in the northern delta like Alexandria, Rosetta, Damietta and Port Said will be submerged by 0.5 SLR (Fitzgerald et al., 2008).

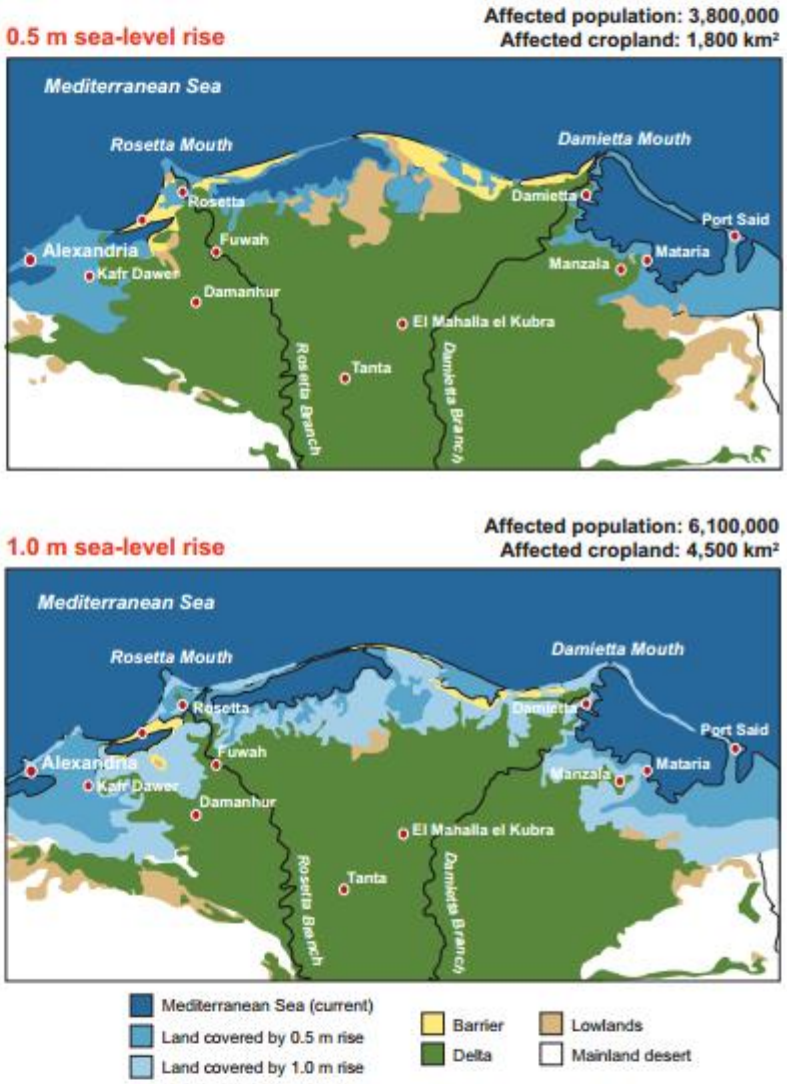


*Figure 7. Effect of different SLR scenarios on the population and croplands of the Nile Delta. (Fitzgerald et al., 2008)*

According to important research on climate change and its impacts on the coastal zone of the Nile Delta (El-Nahry & Doluschitz, 2010), different scenarios (1 m, 1.5 m & 2 m) were constructed for the sea level rise in the area (**Figure** 8). In case of 1 m SLR and 2 mm/year subsidence, 30% of Alexandria will be flooded and parts of offshore protective sand dune barrier will be destroyed, also 28.93% of the Nile Delta will disappear and salinity will intensify in the soil. If it reaches 1.5 m, another 6.39% of the delta will be submerged below the sea and food shortage will happen. On the other hand, a 2-meter SLR will decrease agricultural production by 50% and the major cities on the coast will disappear like Port Said and Alexandria (El-Nahry & Doluschitz, 2010).

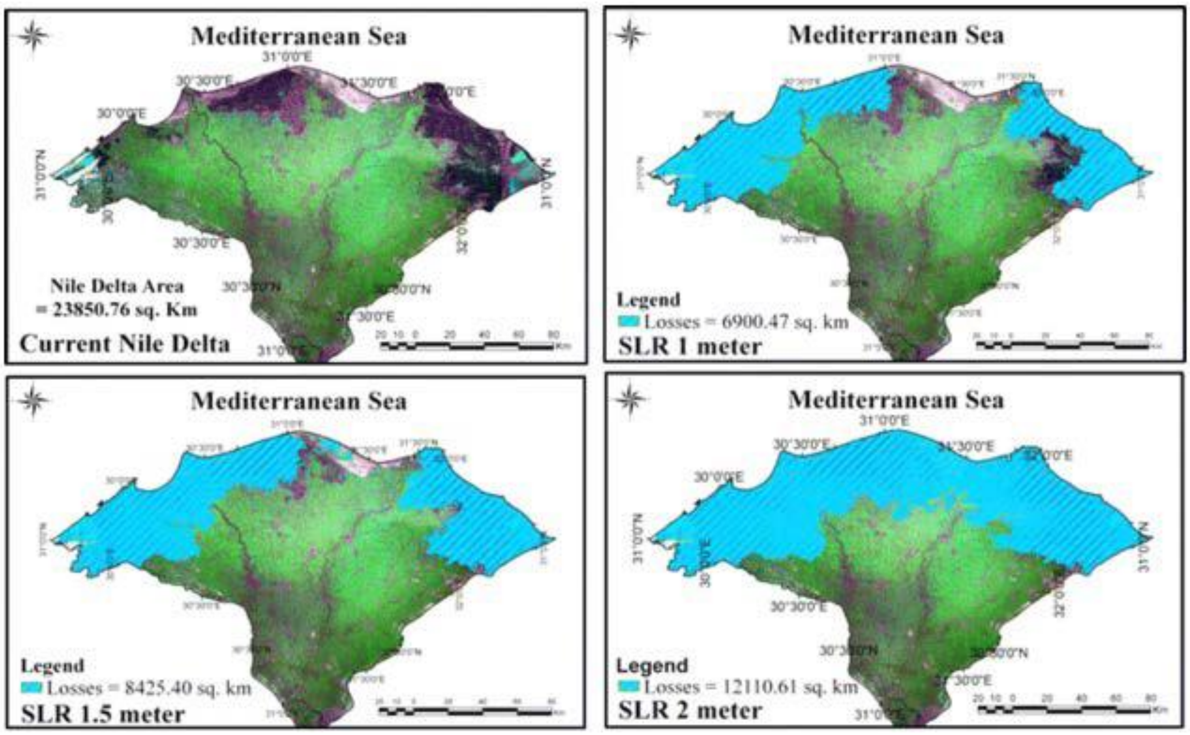


***Figure 8.*** *Different SLR scenarios with total lost areas until year 2100. (El-Nahry & Doluschitz, 2010)*

### 1.4. DEMS and GEBCO Bathymetry

Digital Elevation Model (DEM) is defined as a 3D representation of the terrain's elevation that can be generated using terrestrial surveys, aerial photos, LIDAR, contour elevations, GPS measurements and onboard sensors (**Figure** 9 & 10). Advanced Spaceborne Thermal Emission and Reflection Radiometer Global DEM (ASTER-GDEM) and the Shuttle Radar Topography Mission (SRTM) come amongst the most famous and freely accessed DEM products that provide vital information about the Earth's surface. The SRTM collected radar data over 80% of the Earth's land surface and was released on February 11, 2000, with two types of antenna, C-band and X-band and is available in 2 main resolutions; 1 arc-second (~30 m) spatial resolution and 3 arc-sec (~90 m) for global use (SRTM-DEM, 2006).

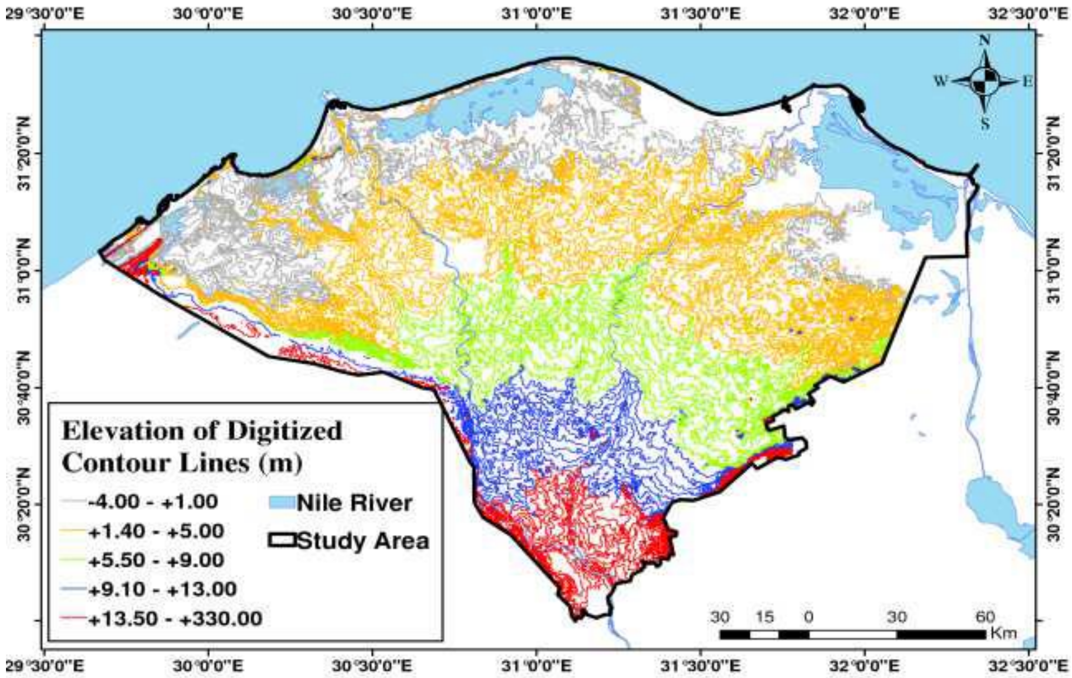


**Figure 9.** *The digitized contour lines from the topographic maps of the Delta region. (El-Quilish et al., 2018)*

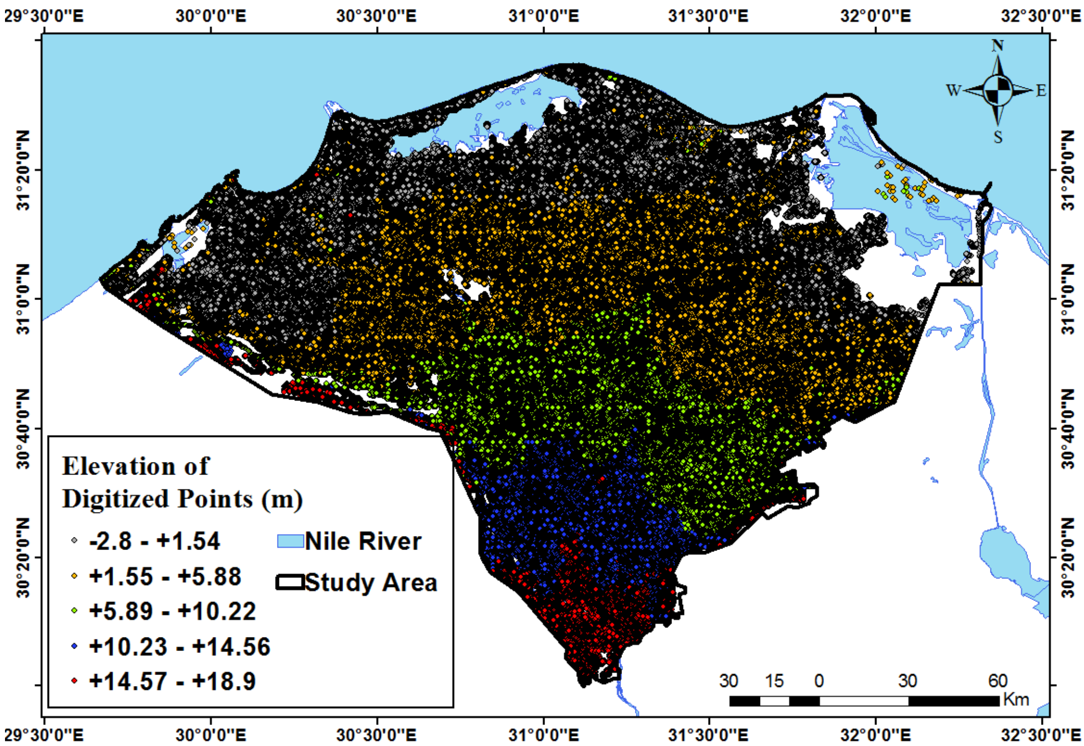


***Figure 10.*** The elevation points from the topographic maps of the Delta region. (El-Quilish et al., 2018)

On the other hand, The ASTER-GDEM is available in 1 arc-second (~30 m) and includes 2 main versions; ASTER-GDEM-V-1 and V-2. The latter's data is much improved from the first version as it removes some of the most common DEM errors like sinks and artifacts (Hasan et al., 2015). This DEM is generated using stereo-pair images of Band 3, the nadir (3N) band and the back-looking (3B) band, collected by the ASTER instrument onboard the Terra mission (ASTER-GDEM, 2011). In **Figure** 11 below, we can see the representation of elevation from the original DEM datasets, where fig. 11a shows how uniform the original SRTM distributed the elevation values that gradually increase as moving from the northern shoreline towards the southern land. On the contrary, fig. 11b shows more elevations recorded by ASTER-GDEM-V-1 that are less uniformly distributed across the Nile Delta.

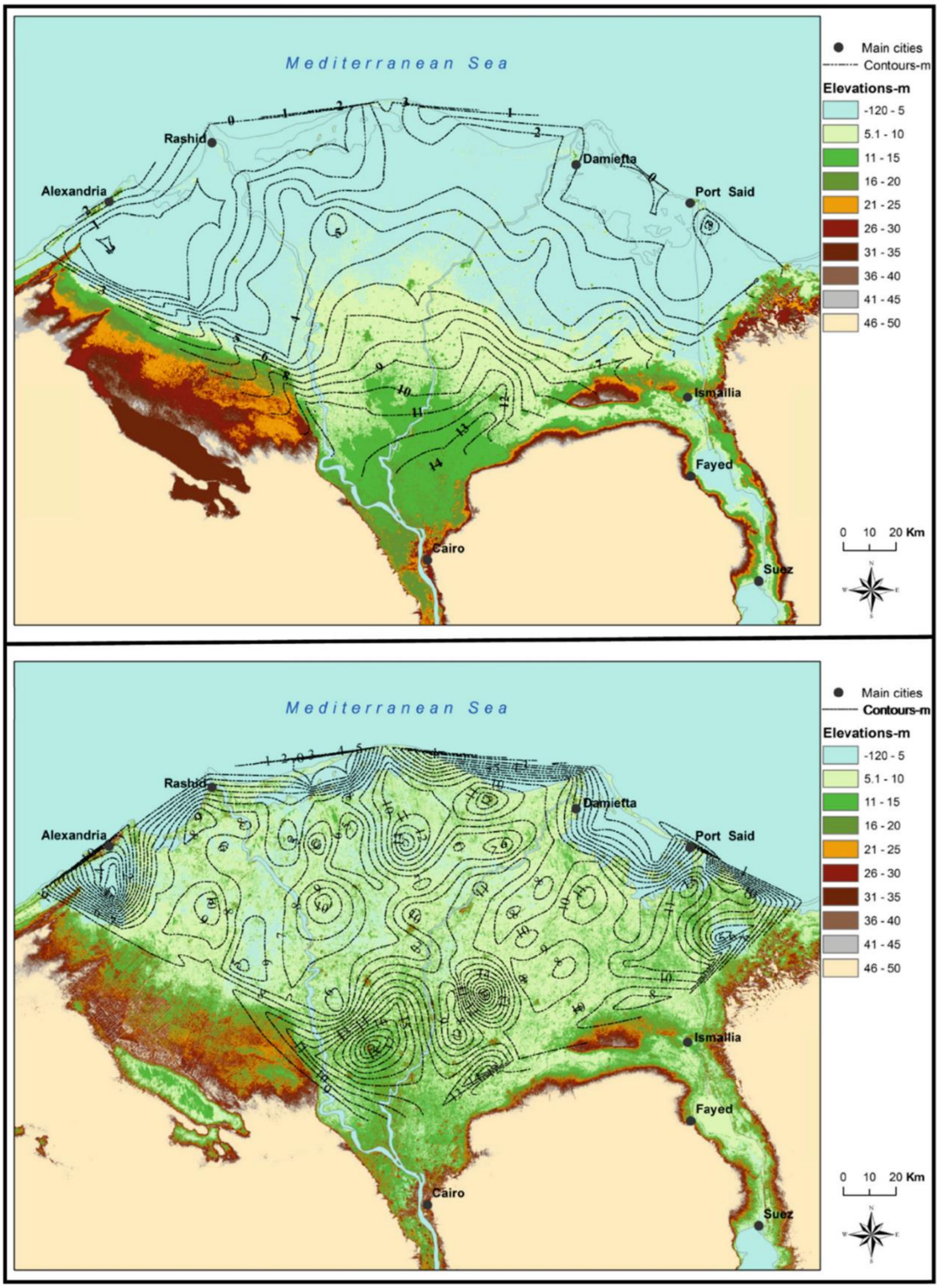


***Figure 11.*** *Contour maps of original DEMs using an interval of 1 m.* ***a*** *the SRTM-DEM shows more homogenous elevations that increase from the north to south, while in* ***b*** *it shows more elevation points and less uniform elevation distribution. (Hasan et al., 2015*

DEMS are generally relevant for many applications such as flood estimation, hydrology and flow-direction studies, land use planning and quantification of earth materials to be moved for roads, dams, channels and embankments (Refaat & Eldeberky, 2016). Their accuracy depends on their spatial resolution and data sources. Terrestrial surveys use both modern and conventional surveying instruments for producing DEMs such as Global Navigation Satellite System (GNSS), leveling and total stations. Despite the fact that this method gives reasonably accurate results, it is less efficient and time-consuming when applied to an area which is not easily accessible (Hussien et al., 2021). LIDAR and aerial surveys produce DEMs with good elevation accuracy that cover large areas compared to terrestrial surveys. Therefore, choosing the right DEMs for an accurate mapping and visualization of the study area (Figure 12) play a key role in geospatial analysis, mainly for investigating the hazardous impacts of SLR and land subsidence phenomena.

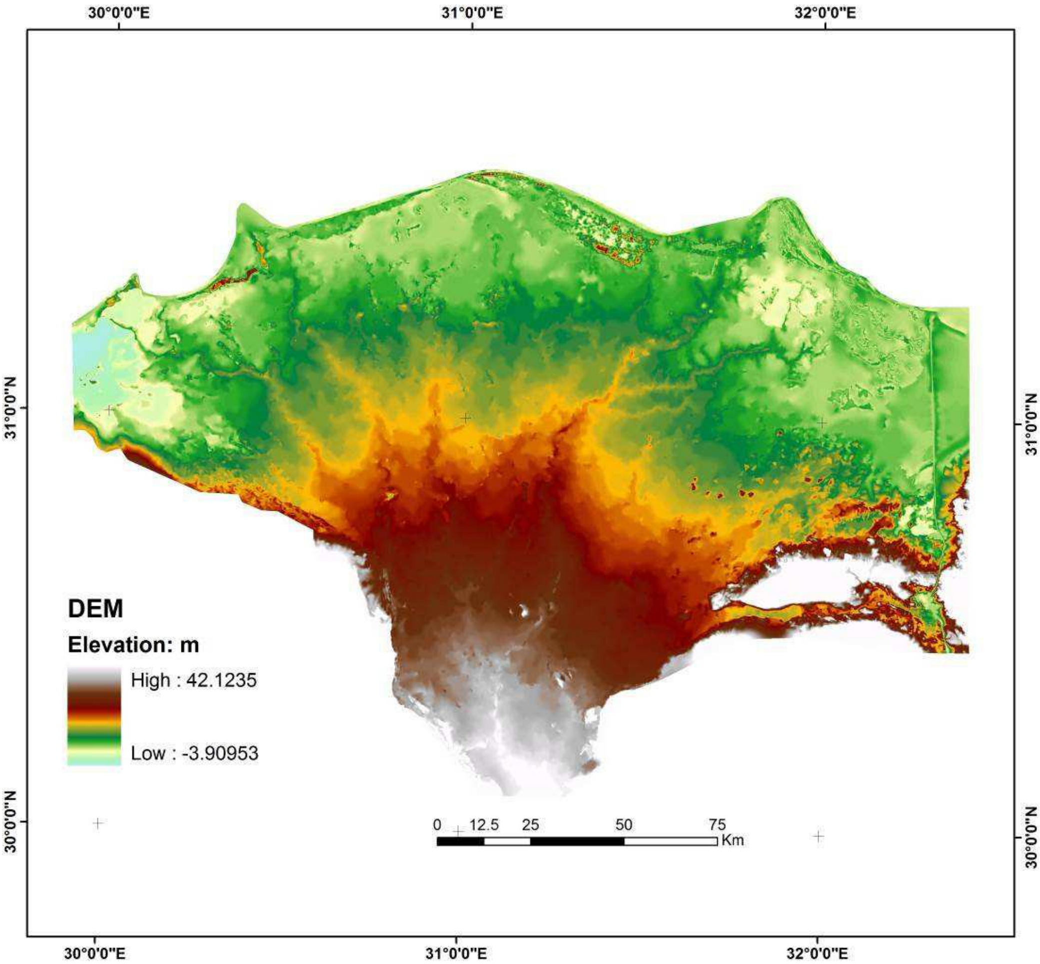


***Figure 12.*** *A DEM of the Nile Delta showing the longitudinal ridges (brown to yellow) which are being inter-fingered by lower terrain areas (green color). (El Bastawesy et al., 2016)*

GEBCO 2022 grid which is the British Oceanographic Data Centre (BODC) current gridded bathymetry dataset is a global terrain model for oceans and lands providing elevation data with spatial resolution of 15 arc-second (~450 m) and accompanied by a Type Identifier (TID) Grid that informs the user about sources of data on which GEBCO 2022 grid is based (GEBCO, 2022). The main aim is providing the most accurate publicly available authoritative bathymetry of the world's oceans with global coverage which can be downloaded as global files in NetCDF format or a set of 8 tiles (each with an area of 90° x 90°) as shown below in **Figure** 12. Global-scale bathymetry is an important factor for geophysical, geological, and oceanographic research. Daniell (2010) concluded that combining remotely sensed bathymetry and GEBCO bathymetry grid can result in more accurate representation of the targeted surroundings in regional or global-scale regions.

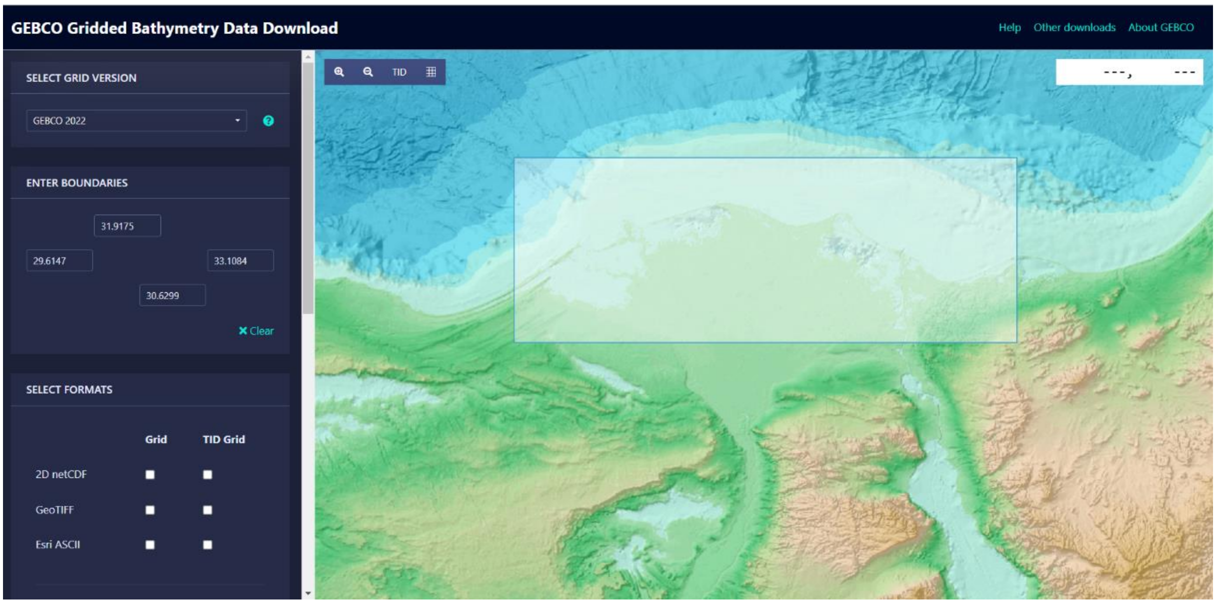


***Figure 13.*** GEBCO gridded bathymetry data download website interface with the Nile Delta area selected. (Screenshot taken by the author)

# 2. LITERATURE REVIEW

Satellite altimetry is a remote sensing technology that utilizes satellite measurements to determine the height of various objects, including the Earth's surface, the sea level, and the height of ice sheets. The measurements are usually characterized by high resolution, global coverage and short revisit time. The accuracy of sea surface height measurements reached the 1-cm level by today, where it has increased by the factor of 100 since the very first missions in the mid-1970s (Cazenave, 2019). It works by measuring the time it takes for a radar pulse emitted from the satellite to bounce off the surface of the Earth and return to the satellite (**Figure** 13). This time measurement, combined with knowledge of the speed of light, allows for the calculation of the height of the surface below the satellite. Such techniques have revolutionized our knowledge of the oceans' dynamics, climate-related SLR and land hydrology.

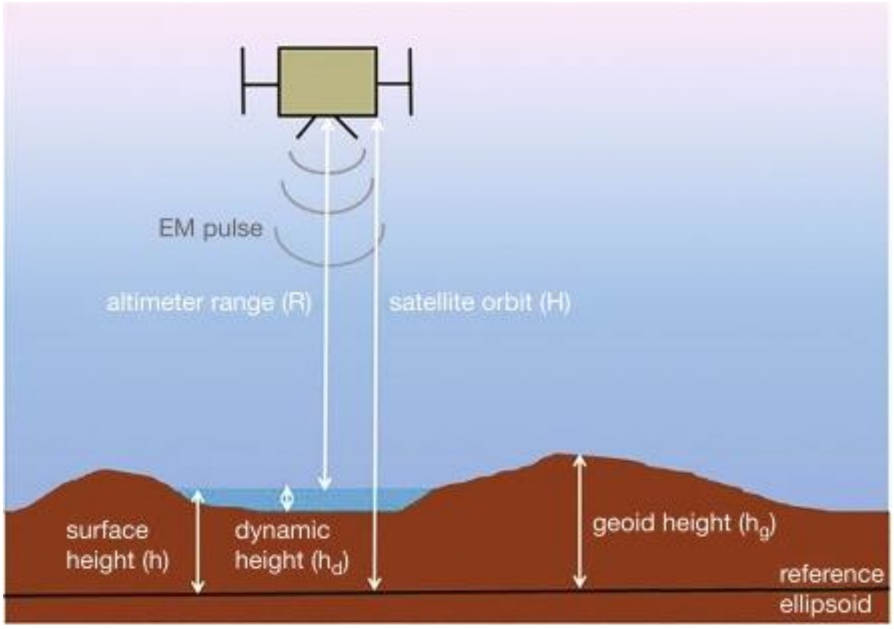


***Figure 14.*** *The principle of radar altimetry measurement. (Cazenave, 2019)*

The first three altimetry missions were initiated from the US, where NASA's Geos-3 was the first satellite using radar altimeter in 1975 until 1978 and afterwards, other missions started to follow from different space agencies like European Space Agency's (ESA) CryoSat (2010) and Copernicus Sentinel-3 that was launched in 2016.

The latter's goal is to measure the sea surface topography, land and sea surface temperature, and ocean and land surface color with high accuracy and reliability that can support climate monitoring and forecasting systems (ESA, 2021). Compared to other missions, CryoSat and Sentinel-3 use synthetic aperture radar (SAR) altimetry that attain higher along-track resolution of sea surface height measurements.

The data obtained from satellite altimetry usually needs to be corrected for various factors due to atmospheric delay, instrumental drifts and bias between successive missions. Solid earth, pole and ocean tides are other corrections due to geophysical effects that should be applied (Cazenave, 2019). It is important to highlight that SRTM is a satellite altimetry mission that uses radar technology to create a detailed high-resolution DEM of the planet. However, other DEMs are not exactly the same thing as satellite altimetry as they are products that can be derived from it. DEMs can be created using satellite altimetry via measuring the height of the Earth's surface at different points and then using interpolation techniques to create a continuous surface model.

### 2.1. Remote Sensing in Coastal Management

The utilization of remote sensing and digital elevation models (DEMs) is imperative in the effective management of coastal regions as they offer vital information on the physical characteristics and activities prevalent within such environments. The use of remote sensing techniques such as satellite imagery and LiDAR provides detailed data on various features including dunes, wetlands, and shorelines. This high-resolution data from different modern technologies (**Table** 1) allows for easy monitoring of changes occurring in the coastal areas (Atkinson & Tatnall, 1997). DEMs are generated from remote sensing data and present precise information on elevation, slope, and topography. This makes them a crucial tool when modeling and comprehending coastal processes (Heinz Center, 2000). According to Luijendijk et al. (2018), DEMs are essential tools in understanding and managing coastal regions, as they provide critical information on topography, elevation, and other physical features that play a role in coastal processes. By using DEMs to model the impacts of sea-level rise and storm surges, we can better prepare for and mitigate the effects of these hazards on coastal environments and infrastructure. Additionally, DEMs with their different resolutions (**Table** 2) help identify areas of high ecological significance in coastal regions, which is important for conservation efforts (Spalding et al., 2014).

| Method | Spatial Scale | Spatial Resolution | Temporal Scale | Temporal Resolution | Accuracy |
|---|---|---|---|---|---|
| Digitized aerial photos / T-sheets | 10-1000 km | ~50-100 m along-shore | Decades | Decades | 1-15 m |
| RTK-GPS / in-situ survey methods (e.g., Emery) | 1-10 km | 0.5 m cross-shore<br>~100 m alongshore | Decades (monitored sites) | Weekly to monthly | 5-10 cm |
| Fixed cameras | ~1 km | 0.5 m – 10 m (near-field to far-field) | Decades (monitored sites) | Minutes to hours | 1-2 m |
| Crowdsourced CoastSnap | ~1 km | 0.5 m – 10 m (nearfield – far field) | 1-3 years | Daily to weekly | 2-4 m |
| Drone SfM | 1-5 km | ~0.5 m | ~5 years | Monthly to yearly | ~0.5 m |
| Aerial photogrammetry | ~100 km | ~0.5 m | Decades | 1-5 years | 1-5 m |
| Airborne Lidar | ~100 km | ~0.1 m | Decades | Yearly | ~0.5 m |
| Earth Observation Satellites (Landsat/Sentinel-2) | Global | 1 m-30 m | 36 years | Daily to Bi-weekly | ~10-15 m |
| Cubesats (PlanetScope) | Global | 3 m | 5 years | Daily | ~5 m |

***Table 1.*** *A summary of different modern technologies for shoreline monitoring. (Vitousek et al., 2023)*

| GDEM | Full Name | Released Year | Spatial Resolution | | Download from |
|---|---|---|---|---|---|
| | | | arc second | m | |
| AW3D30 | The Advanced Land Observing Satellite | 2015 | 1” | ~30 | https://www.eorc.jaxa.jp/ALOS/en/aw3d30/ |
| SRTM 1 | Shuttle Radar Topography Mission | 2015 | 1” | ~30 | https://earthexplorer.usgs.gov/ |
| ASTER v.2 | Advanced Space borne Thermal Emission and Reflection Radiometer | 2011 | 1” | ~30 | https://asterweb.jpl.nasa.gov/gdem.asp |
| EARTHEnv-DEM90 | - | 2014 | 3” | ~90 | https://www.earthenv.org/DEM |
| SRTM 3 | Shuttle Radar Topography Mission | 2009 | 3” | ~90 | https://srtm.csi.cgiar.org/ |
| GMTED2010 | Global Multi-resolution Terrain Elevation Data 2010 | 2011 | 7.5” | ~225 | https://topotools.cr.usgs.gov/gmted_viewer/viewer.htm |
| GLOBE | Global Land One-km Base Elevation | 2000 | 30” | ~900 | https://www.ngdc.noaa.gov/mgg/topo/globe.html |
| GTOPO30 | Global 30 Arc-Second Elevation | 1996 | 30” | ~900 | https://earthexplorer.usgs.gov/ |

***Table 2.*** *Characteristics of the different global DEMs. (El-Quilish et al., 2018)*

## 2.2. DEMs: Advantages and Limitations

Utilizing remote sensing and DEMs can prove advantageous in the development and preparation of coastal infrastructure, such as ports, harbors, and seawalls. These tools furnish engineers and planners with comprehensive insights into the coastal environment, extending from elevation to slope and vegetation coverage. With such vital information at their disposal, designers can create infrastructure that is capable of enduring various coastal hazards (Parris et al., 2012). Additionally, Zhang et al. (2016) mentioned that remote sensing data demonstrates its usefulness in tracking the effect of constructed coastal infrastructure on the surrounding habitat - notably observed through alterations in sediment transport or erosion patterns.

However, Satellite-derived DEMs have certain limitations, the most significant being their data quality. The accuracy of DEM data is crucial for various applications such as terrain modeling and analysis, but it is dependent on multiple factors, including the method used for data acquisition, processing techniques employed during data handling, as well as the characteristics of the terrain being mapped. Therefore, it becomes vital to take into account these factors while evaluating a satellite-derived DEM's quality and its suitability for specific applications (Musa et al., 2015).

Satellite-derived DEMs typically have lower vertical accuracy, higher bias, and higher root-mean-square error (RMSE) compared to other DEMs derived from LIDAR and InSAR (Fraser & Ravanbakhsh, 2011). This is because satellite sensors are farther away from the Earth's surface than airborne sensors, resulting in lower resolution data. Despite their lower accuracy compared to other DEMs, Gorokhovich and Voustianiouk (2006) and Karlsson and Arnberg (2011) agreed that satellite-derived DEMs can still be useful sources of topographic data for low-lying coastal areas with gentle slopes which makes them practical for inundation modeling. Therefore, the utilization of remote sensing and DEMs is incredibly significant in coastal management. These tools offer crucial insights into various aspects related to the coastline such as natural processes, potential risks, and resources available in the surrounding area. Having access to such information is vital for managing and mitigating the impacts of coastal hazards, as well as safeguarding coastal ecosystems and communities from the adverse effects of global climate change and rising sea levels. Therefore, it is essential that decision-makers and stakeholders prioritize these tools in their efforts to promote sustainable coastal development practices.

### 2.3. Potential Impacts of SLR and Land Subsidence on Nile Delta

The Nile Delta in Egypt due to its land topography (**Figure** 15) is expected to encounter a SLR of 1 m maximum by the end of this century (Dasgupta et al., 2009; Fitzgerald et al., 2008; Eldeberky & Hünicke, 2015) and to conduct a more accurate assessment of this upcoming SLR impact on the Nile Delta's land and its population, the focus has to be more on utilizing DEMs elevations using statistical models and predictive analysis along with ground elevations from GPS and other onsite techniques (Hasan et al., 2015). The aforementioned researchers came up with insightful outcomes in their study using SRTM DEM that about 3900 km2 of cropland, 1280 km2 of vegetation, 146 km2 of urban areas and 205 km2 of wetlands will be affected by only 1 m SRL and around 6 million people will lose their houses.

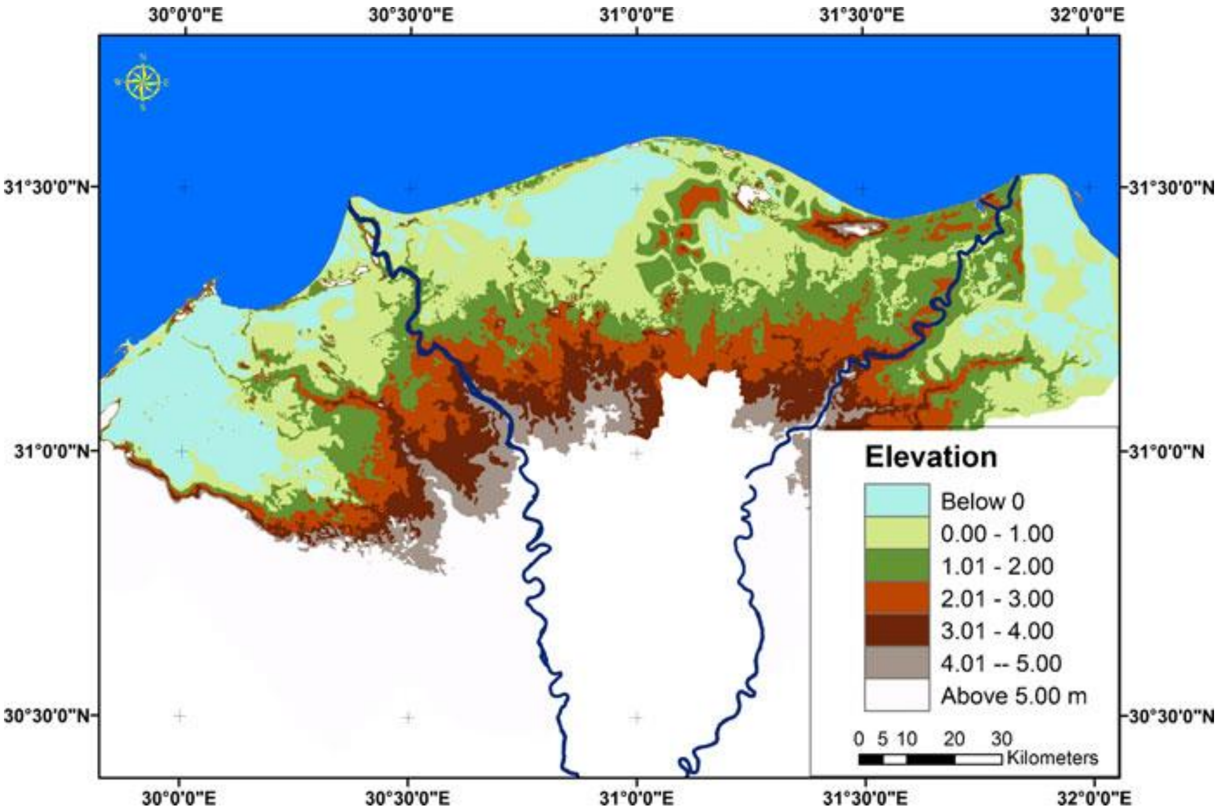


*Figure 15. The land topography of the Nile Delta, Egypt. (Hassaan & Abdrabo, 2012)*

Hereher (2010) confirmed these results as well in his paper regarding the vulnerability of the delta to SLR and estimated that 30.8% of the delta will be flooded, also will result in shoreline erosion, contamination of surface courses and loss of productive agricultural lands. In the same research, it was also mentioned that 2-m SLR will be catastrophic as around 8789 km2 (43.9%) of the delta would be submerged and more than 8 million inhabitants in the four main coastal cities (Alexandria, Damietta, Kafl El-Sheikh and Port Said) will be forced to abandon their homes. Not only that, but also more than 15 million people in other 3 cities (Beheira, Dakahlia and Sharqia) will have to be relocated southwards. Elshinnawy and Almaliki (2021) concluded that another consequence of the SLR in the delta by the end of this century is that the shoreline will experience a retreat between 40 and 160 m with 1.2 m/year average rate. They mentioned for instance that the rising groundwater level will significantly affect 60% of the Gamasa Ras El Bar which is one of the most vulnerable coastal areas in the delta (**Figure** 16).

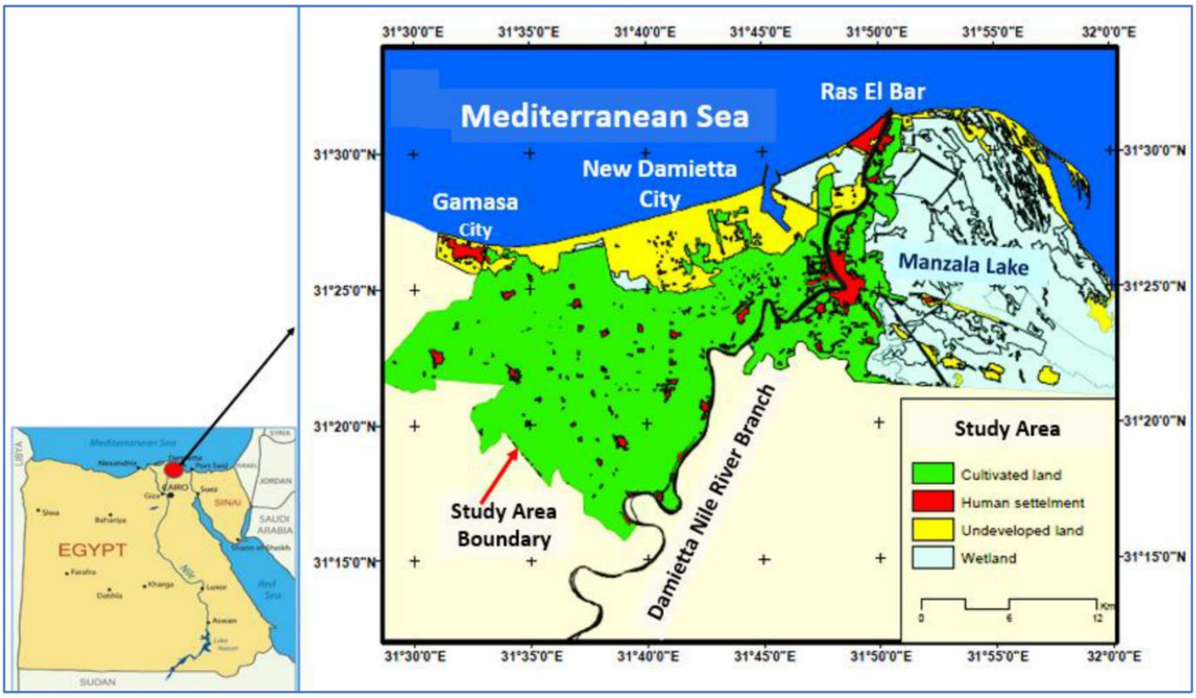


***Figure 16.*** *A map that shows the investigated classified land of the Gamasa Ras El Bar area in the Nile Delta. (Elshinnawy & Almaliki, 2021)*

Not only that, but it will also boost the freshwater-saltwater interface inland by 1 km. This area proved that such a key factor which is one of the SLR consequences would increase the stress on the drainage systems, resulting in water logging and having unfavorable impacts on the whole infrastructure and building foundations in the area.

Regarding land subsidence that some of the delta regions experience, it was found that 15.56% of the total regions of Nile Delta would be vulnerable to inundation because of subsidence only even if the absence of any SLR as shown in **Figure** 17 below (Hassaan & Abdrabo, 2012). In a research where GPS data was used, it was revealed that the Northern part of the Nile Delta is experiencing subsidence, including cities like Port Said, Mansoura, and Alexandria, particularly on the eastern and western sides, while the central part of the region and the surrounding areas are experiencing uplift (Elsaka et al., 2020). Based on another vulnerability analysis of the Nile Delta-Alexandria coast to SLR, it was found that safe areas include the artificially (15%) and naturally protected areas (55%), where the areas (30%) that are at high risk are the low-lying and narrow sandy lagoon barriers of the Burullus and Manzala lagoons (Frihy, 2003). He also found that long-term land subsidence can have a crucial role based on statistical analysis of long-term tide gauges data recorded at Burullus, Alexandria and Port Said with values of 1, 1.6 and 2.2 mm/year respectively. Moreover, intensified storm surges could significantly impact the lower Nile Delta, mainly parts of Alexandria and Port Said in terms of low-lying land submergence and coastal barriers breaching (Eldeberky & Hünicke, 2015).

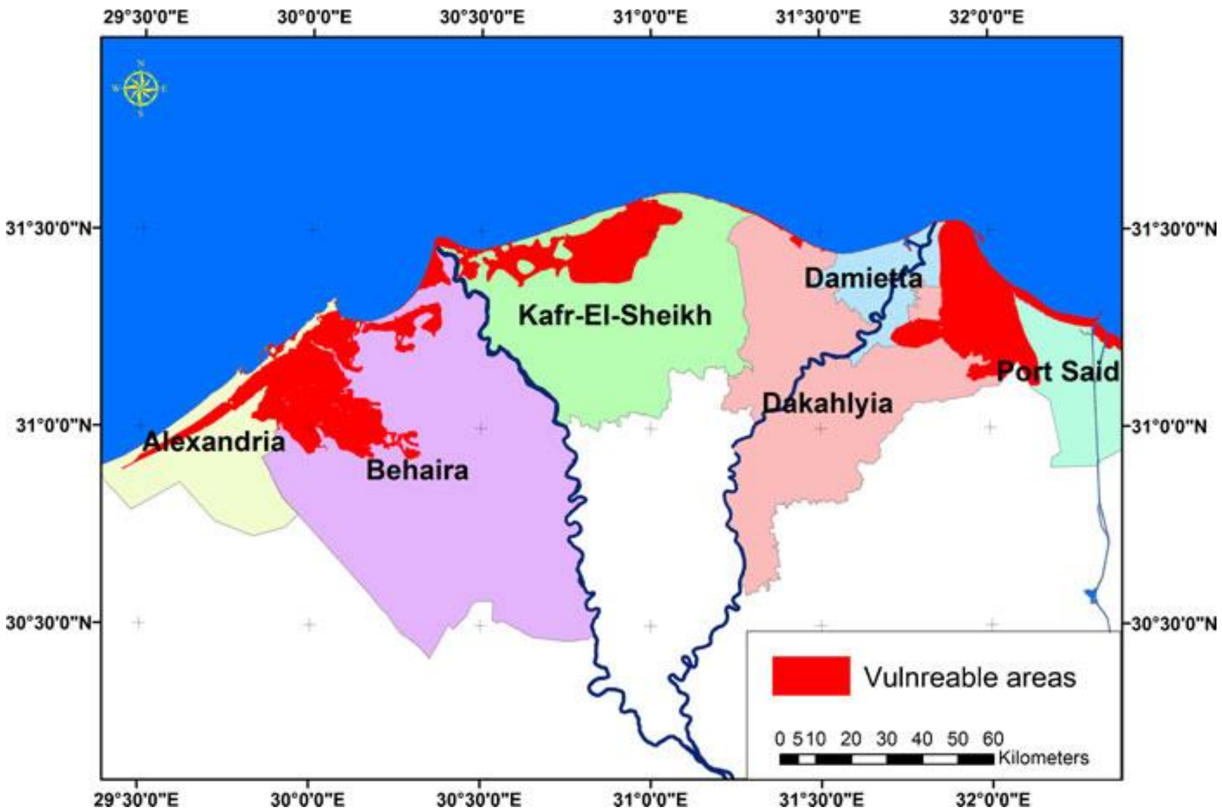


*__Figure 17.__ The Nile Delta map showing the most vulnerable areas to inundation due to land subsidence by 2100. (Hassaan & Abdrabo, 2012)*

When we talk about SLR impacts on the Nile Delta due to its land topography with different SLR scenarios, we are talking about high vulnerability and significant socio-economic loss. The increasing population growth, socioeconomic changes, and agricultural expansion in the Nile Delta are expected to put pressure on water resources. This may lead to an increased reliance on groundwater sources, which could exacerbate problems such as seawater intrusion and damage to infrastructure in cities like Alexandria (Sefelnasr & Sherif, 2013). The coastal cities in the delta are at high risk of 50 cm SLR that can result in displacement of around 2 million inhabitants and loss of about 215,000 jobs and over 30 billion of value loss only in Alexandria city (El-Raey, 1997). Hassaan and Abdrabo (2012) classified the 6 coastal governorates of the Nile Delta into two categories based on areas vulnerable to inundation due to SLR; highly vulnerable governorates that include Port Said, Kafr El-Sheikh and Damietta located in the eastern part of the delta and less vulnerable ones including Alexandria, Dakahlia, and Beheira. The potential impacts on the coastal zone of the Nile Delta from different SLR are summarized in **Table** 3 below and visually in **Figure** 18.

| SLR Scenario | Land submerged (Square kilometers) | Percentage of land submerged | No. of People affected |
|---|---|---|---|
| 0.5m SLR | 1800 | 7.5% | 4 million |
| 1.0m SLR | 4500 | 18.9% | 6.1 million |
| 1.5m SLR | 5700 | 23.9% | 8 million |

***Table 3.*** *Summary of the potential land loss and people affected from different SLR scenarios. (Eldeberky, 2011)*

Unfortunately, the loss of beaches will reduce the number of tourists and affect the tourism sector badly, which in return will impact the employment rate badly. The crop yield will also be reduced causing agricultural disruption of crops which can lead to desertification. According to the world bank report, Port Said city was found to be the first in North Africa and the Middle East to be affected by SLR. The beach areas will be mostly affected, followed by urban areas, where the agricultural sector will be the least affected (El-Raey et al., 1999).

The previously mentioned paper also estimated the economic loss in Port Said to be over 2 billion dollars for 0.5 m and might exceed 4.4 billion for 1.25 m SLR, also around 28,000 to 70,000 people would be expected to be displaced and approximately 6,700 to 16,700 jobs will be lost.

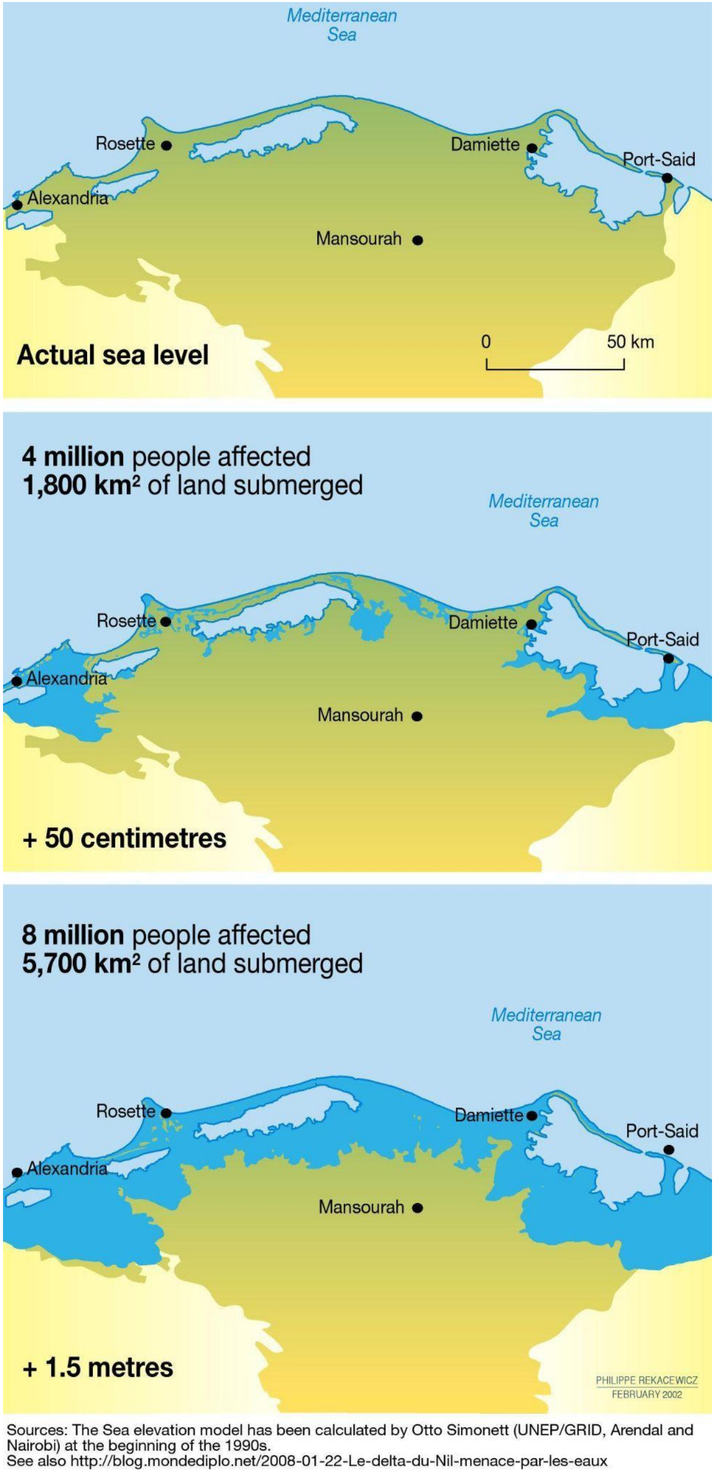


***Figure 18.*** *Expected impacts of 0.5 and 1.5 m SLR on the Nile Delta. (Rekacewicz & Simonett, 1990)*

# 3. METHODOLOGY

The data utilized in this work was provided by the BODC which represents GEBCO bathymetry data for the study area generated by combining quality-controlled ship depth soundings with interpolation between sounding points guided by satellite-derived gravity data. The other dataset was provided by NASA and the National Geospatial-Intelligence Agency (NGA) and represents SRTM Version 3.0 Global 1 Arc-Second (SRTMGL1). Generally, the accuracy of elevation information is the factor on which the delineation of SLR-induced inundated regions depends in such assessments and many studies were conducted to assess the reliability and accuracy of DEMs in environmental applications in general and SLR impact assessment in particular (Abdel-Aziz et al., 2020). ArcGIS Pro 3.1.1 software provided by ESRI was used to process and analyze the DEMs and perform the geospatial analysis to come up with the results that will be discussed later in the next chapter.

## 3.1. Description of the Study Area

The investigated coastal study area represents the northern Nile Delta along the Mediterranean Sea sector that extends from 29°15’E to longitude 32°42’E, and from latitude 30°37’N to latitude 31°35’N (**Figure** 19). The length of the study area is approximately 110 km from north to south with an extent of 345 km from Port Said at the east to Alexandria to the west and an overall area of about 26,470 km$^2$. According to the Central Agency for Public Mobilization and Statistics (CAPMAS), the Nile Delta is considered as one of the most densely populated regions worldwide with more than 50 million people and the table below gives a comprehensive image of the population explosion of the governorates that make up the AOI in 2022 (**Table** 4). The WGS1984 UTM Zone 36N was chosen to be the map projection for the study area as the UTM projection is usually used for mapping and surveying purposes worldwide. This projection is suitable for a country’s geography like Egypt as it is mostly located in the Eastern Hemisphere, with a large part of its area lying within the UTM Zone 36N. Therefore, it ensures accurate location and representation of features on the map geographically without considerable distortion.


*Figure 19.* *A high-res Maxar satellite image for the study area. (Created by the author in ArcGIS Pro)*

| Governorates | Population (millions) |
|---|---|
| Alexandria | 5.5 |
| Beheira | 6.8 |
| Dakahlia | 7 |
| Damietta | 1.6 |
| Gharbia | 5.4 |
| Ismailia | 1.4 |
| Kafr El-Sheikh | 3.7 |
| Port Said | 0.8 |
| Sharqia | 7.9 |

*Table 4.* *Population of governorates that comprise the northern delta in 2022. (Obtained from CAPMAS, http://www.capmas.gov.eg/)*

The land use map for the northern Nile Delta has been extracted from Sentinel-2 10-m land Cover Explorer (https://livingatlas.arcgis.com/landcoverexplorer/) data powered by Esri (**Figure** 20) via reclassifying classes based on unique raster values. This is a newly released application from Esri, in partnership with Microsoft and Impact Observatory showing the land use/land cover data of the world in the past six years. Such maps have extreme importance for decision makers in multiple industry sectors and developing nations worldwide. They give us information that help inform policy and management decisions by better quantifying and understanding the impacts of human activities and earth processes. In this case study, the land use map gives us a key aspect in terms of most affected areas in case of different SLR scenarios which will be mainly croplands followed by urban areas.

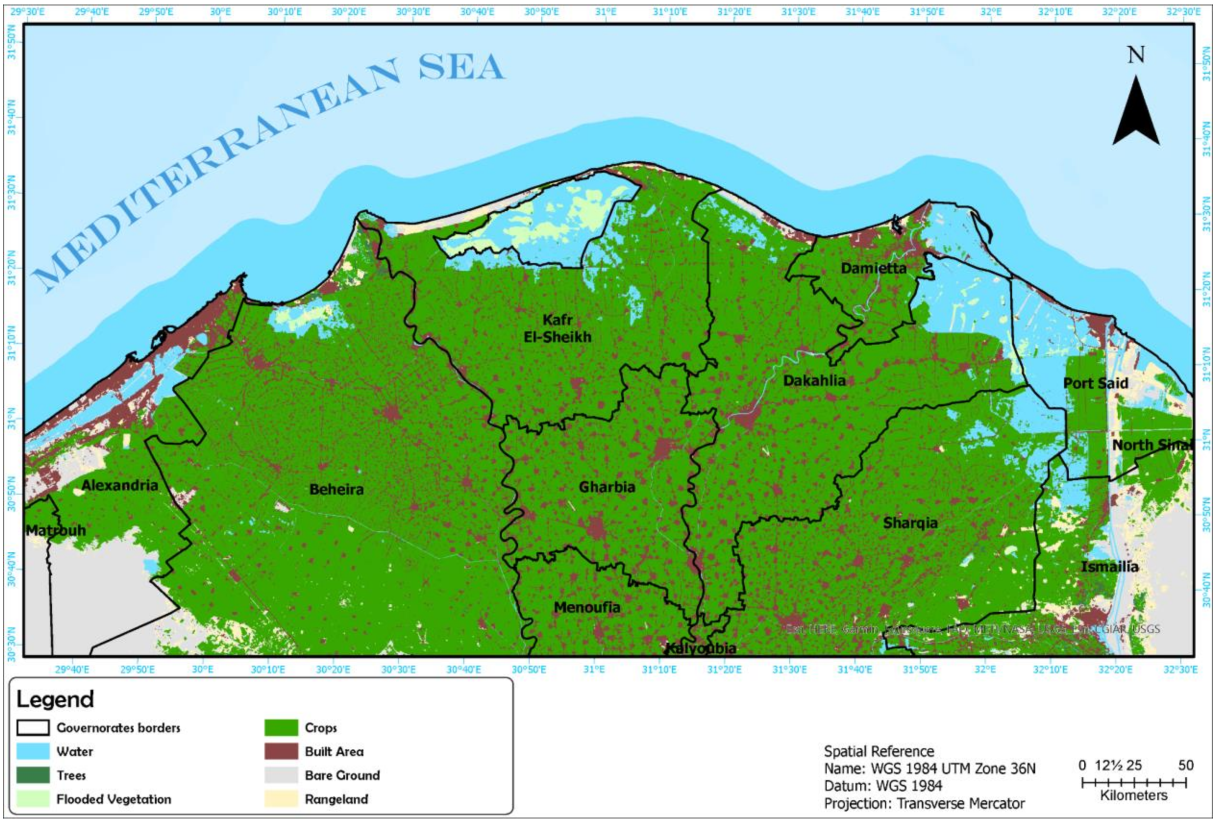


*Figure 20. The land classification of the northern Nile delta based on the classification of Sentinel-2 land cover explorer in 2023. (Created by the author in ArcGIS Pro)*

## 3.2. DEMs Acquisition

SRTM was released in 2000 and it flew for 11 days with the purpose of generating a near-global DEM of the Earth using interferometry. The data is collected in swaths that extend from ~30 degrees off-nadir to ~58 degrees off-nadir from an altitude of 233 kilometers (km) with ~225 km width which comprises 80% of total Earth's land mass. SRTMGL1 data consists of tiles where each contains a mosaic and blend of elevation generated by averaging the data that falls within and these files come in the ".HGT" extension, meaning height (such as N37W105.SRTMGL1.HGT) (NASA JPL, 2013). This version 3 SRTM data that was used in this research was created with the primary goal of eliminating voids that were present in earlier versions, where existing topographic data to replenish SRTM data to fill the existing voids.

Eight SRTM tiles with 16-bit signed integer pixel depth and short pixel type were downloaded as zipped SRTM HGT files at 1-arcsecond resolution (3601x3601 pixels) in a latitude/longitude projection (EPSG:4326) from https://dwtkns.com/srtm30m/ which is a web-based application created by Derek Watkins that requires a NASA Earthdata login to download the files. The SRTM data was validated by scientists using the Kinematic Global Positioning System Geodetic field surveying method as it facilitates the rapid long lines of precise positions from a moving vehicle. NGA geodesists, NASA scientists and private contractors conducted the actual survey work to model the long-wavelength error sources.

On the other hand, 2022 GEBCO bathymetry DEM was downloaded in ".TIF" format with 15 arc-second spatial resolution with the study area defined boundaries from https://download.gebco.net/. The GEBCO DEM comprises data from various resources, including ship-based soundings, satellite altimetry, and airborne surveys to create a global comprehensive dataset of seafloor topography. Not to mention the information it provides on water and land elevation as well with a depth range of -10,800 meters to 8,184 meters. It can be widely used in scientific applications, like geology, marine biology, oceanography and navigation.

Validation and testing the accuracy of any DEM is always a key factor in any kind of similar assessments and analysis, that is why the International Hydrographic Organization (IHO) in 2019 conducted a validation campaign of the latest version of GEBCO DEM. Its aim was to compare GEBCO 2019 dataset to multibeam echo sounder data from various regions of the world's oceans. The results showed that the vertical accuracy of 2019 GEBCO DEM is typically within 1-2% of the water depth, which is considered as highly precise for a global dataset of this magnitude.

## 3.3. Workflow and Geospatial Analysis

This subchapter is dedicated to give a grounded description for the workflow (**Figure** 21) that was implemented in the research and geospatial analysis tools that were used. SRTM and GEBCO bathymetry data was downloaded and imported into ArcGIS Pro, Esri’s most famous full-featured Geographic Information System (GIS) software that enables exploring, visualizing and analyzing data, along with creating 2D maps and 3D scenes. It is important to mention that the 4 different scenarios of SLR were applied to each DEM individually and the results will be further discussed in the last chapter of this work.

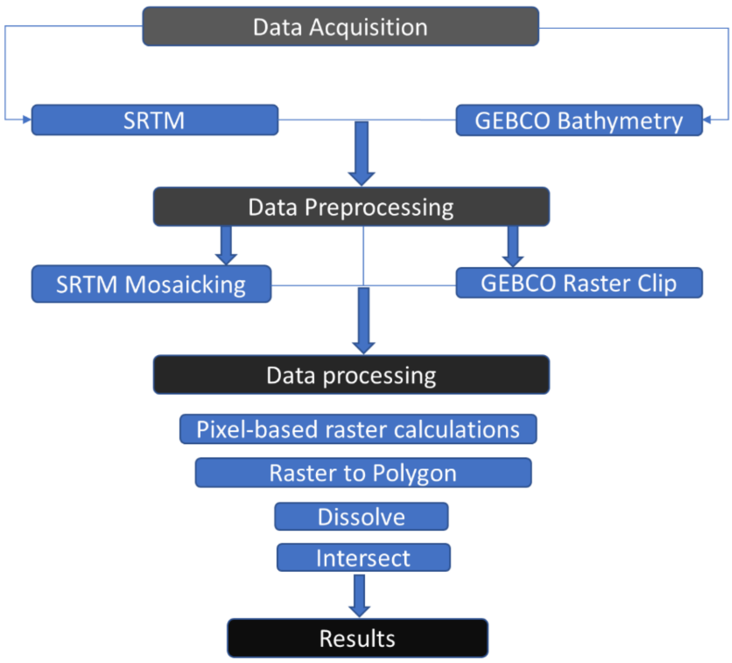


***Figure 21.*** *The workflow chart of the research. (Created by the author)*

First step was data acquisition where both SRTM (8 tiles) and GEBCO (1 TIFF grid) data was downloaded and imported into ArcGIS Pro, along with the the “.SHP” file of Egypt governorates that have attributes like governorates names and their total areas in square kilometers. Afterwards, SRTM tiles were mosaicked into one raster, and along with GEBCO grid they were both clipped by extent to the study area of the northern delta and symbology was changed using same stretch primary symbology and standard deviation type with a vivid elevation color scheme for better visualization (**Figure** 22 and 23).

Then the raster calculator came into the picture to perform the pixel-based calculations in both DEMs using Python syntax and extract only the pixels that meet the criteria of our research for different SLR scenarios (1, 2, 3 and 4 m). After getting the 4 scenarios for each DEM, other conversion, data management and analysis geospatial tools that will be discussed below were utilized for having the final insights and calculate the areas of inundated areas in each governorate in the northern delta. The main geospatial tools for attaining the final results are described briefly below as follows:

1. **Raster to Polygon**: This tool within ArcGIS Pro is one of the most commonly used tools in geospatial analysis as it enables converting the raster images to polygon features.
2. **Intersect:** An analysis tool that calculates the geometric intersection of the input features selecting only those features or parts of features that overlap in all layers or feature classes and creates a new output feature class containing them.
3. **Dissolve:** This data management tool was used for the final step in the geospatial analysis to aggregate the features based on specific attributes. Its role was to assemble the total inundated areas represented by the same governorate where null values are excluded from all statistical calculations.

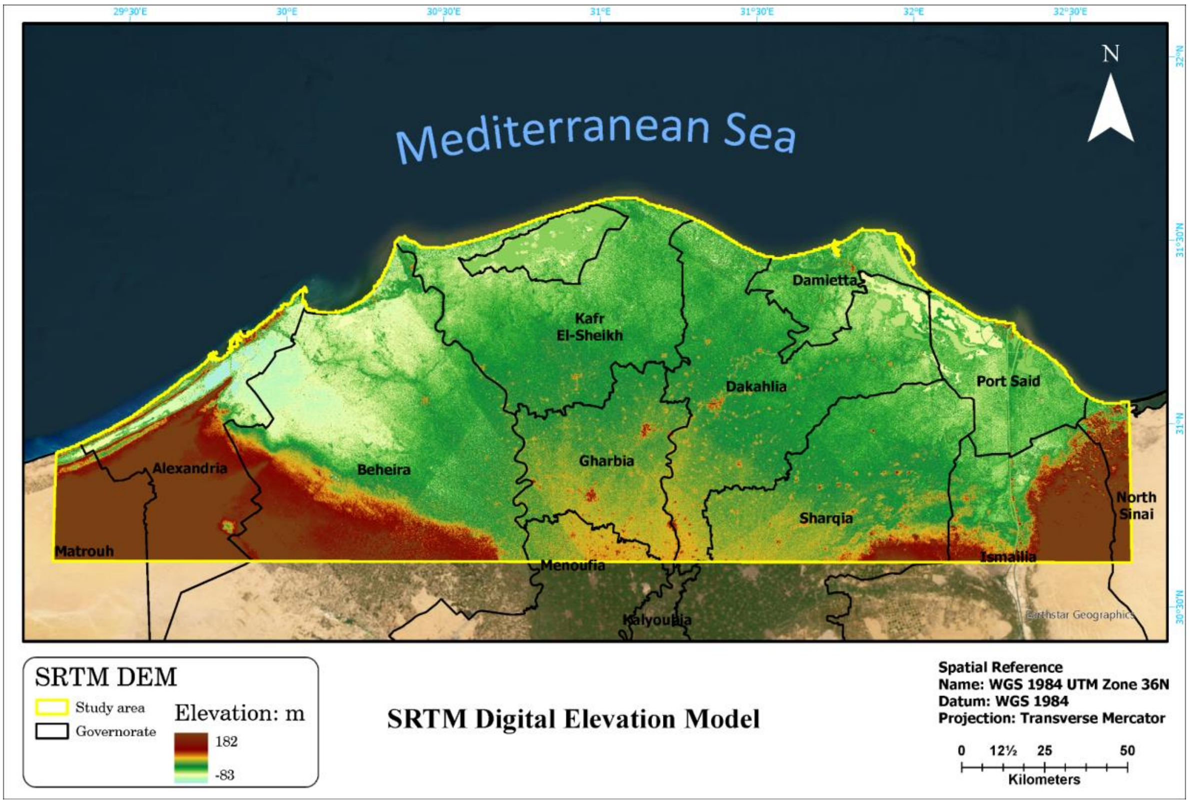


***Figure 22.*** *The SRTM DEM of the study area in the northern delta. (Created by the author in ArcGIS Pro)*

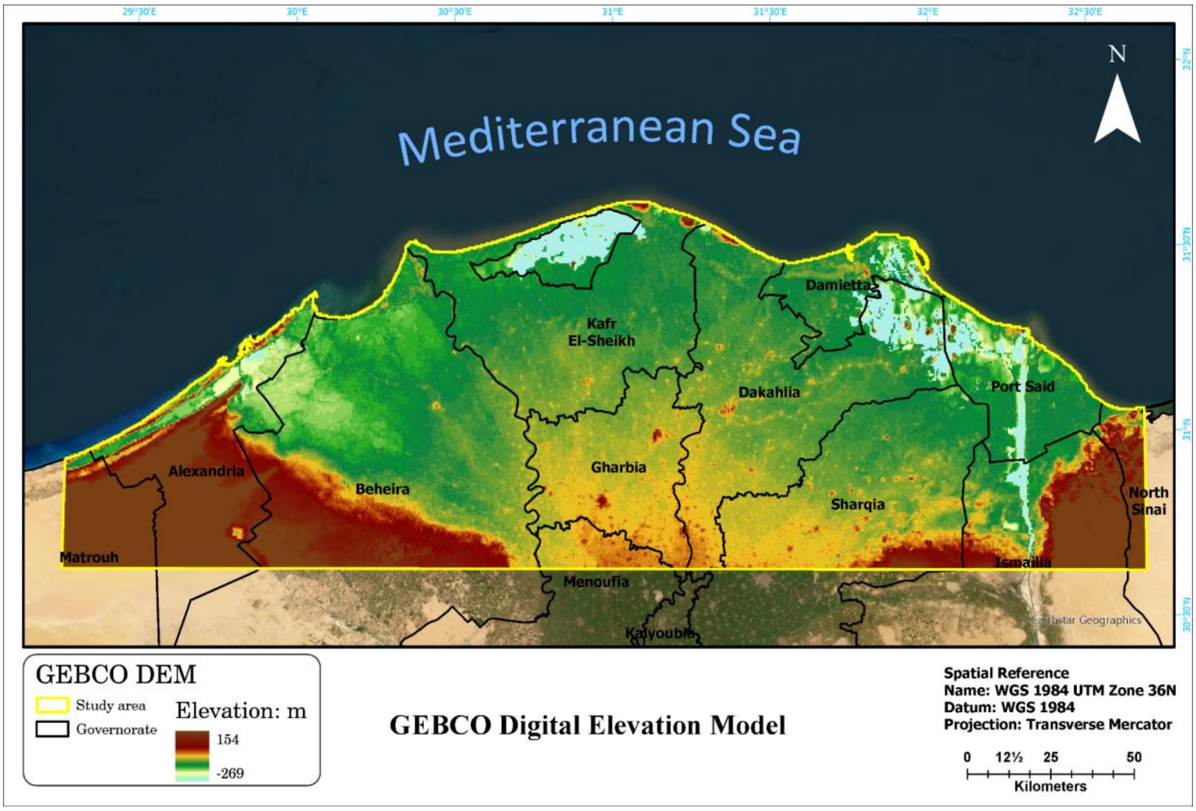


***Figure 23.*** *The GEBCO DEM of the study area in the northern delta. (Created by the author in ArcGIS Pro*

# 4. RESULTS AND DISCUSSION

The accuracy of elevation information utilized in such assessments is usually the factor on which monitoring the SLR-based inundated areas rely. In this chapter, the results of the GEBCO and SRTM DEMs SLR scenarios analysis will be showcased and compared to one another to determine the vulnerable areas to submergence by future SLR in 2050 and beyond. Also, it will highlight the most affected land use types and their total area in each SLR scenario.

## 4.1. GEBCO SLR Scenarios

After the geospatial analysis was performed on the study area using the GEBCO DEM, an overview map was created showing the expected total inundated area in case of future SLR of the four scenarios (**Figure** 24). Accordingly, four maps for each SLR scenario (1, 2, 3 and 4 m) were created showcasing the expected total inundated area in each case and the following tables of each scenario will show the most affected governorates in each scenario with their total inundated areas and total areas (based on CAPMAS data) in square kilometers.

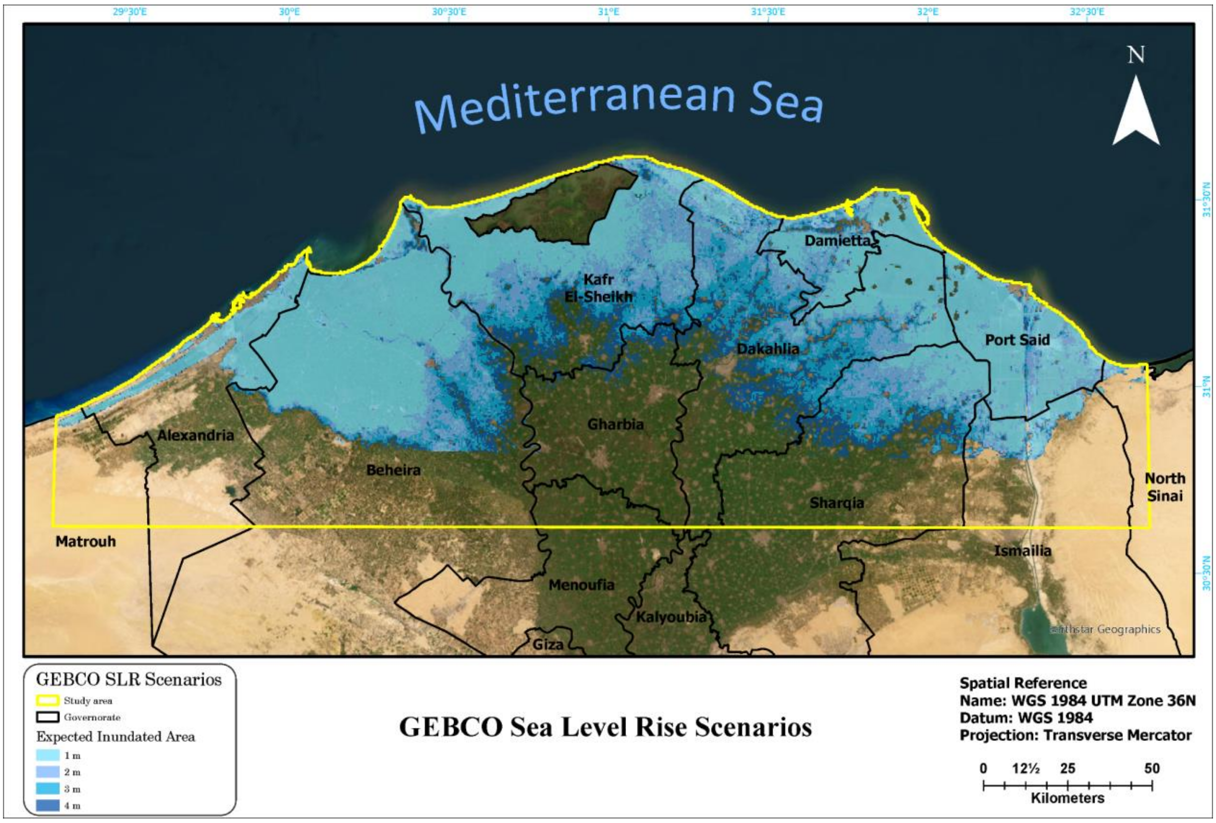


***Figure 24.*** *An overview map for the 4 GEBCO SLR scenarios. (Created by the author in ArcGIS Pro)*

In case of 1 m SLR, major parts of Alexandria, Beheira, Dakahlia, Damietta, Kafr El-Sheikh and Port Said will be first inundated due to their topographic low-land nature and land subsidence (**Figure** 25) with 6,923 km$^2$ total inundated areas. 20% of Alexandria will be inundated, while more than half of Port Said will be submerged as it is the most impacted governorate by the SLR. The following table (**Table** 5) shows the total expected submerged areas in each governorate and their total areas.

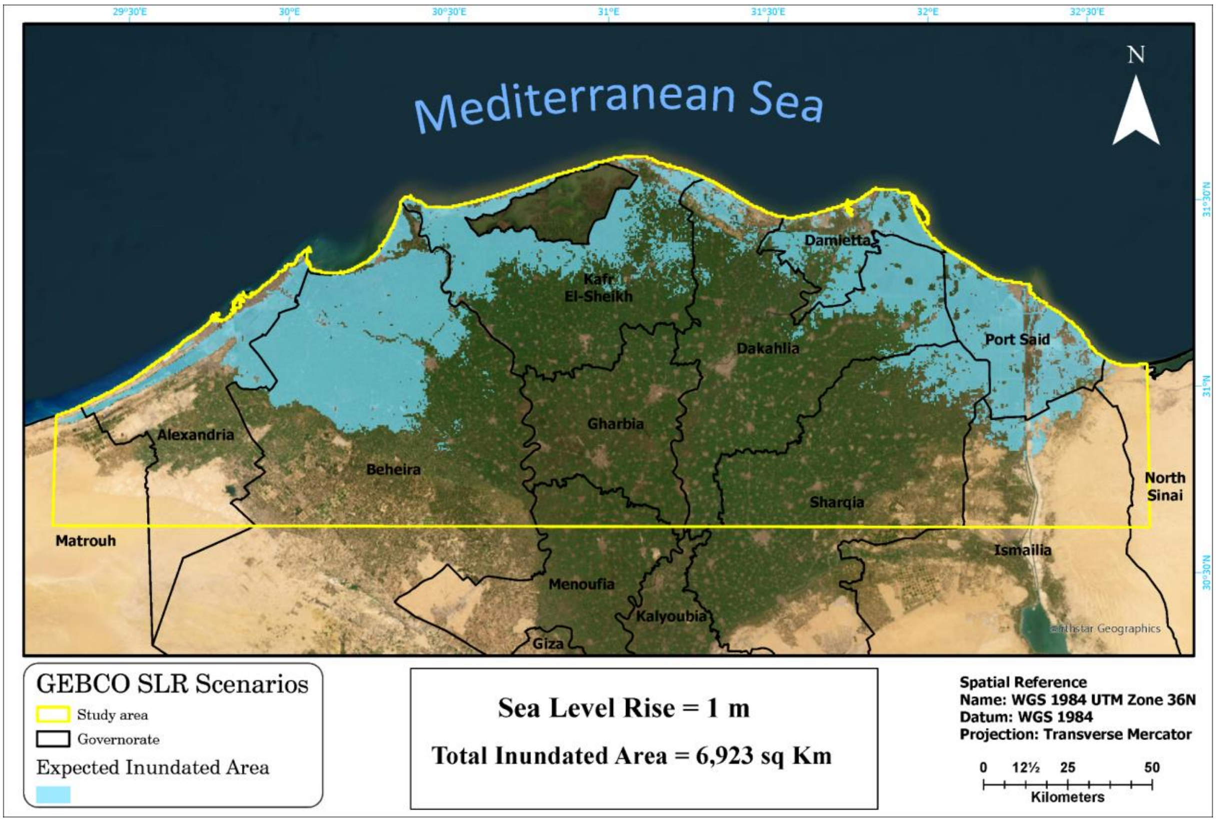


*Figure 25.* *An inundation map of 1 m SLR with the affected areas. (Created by the author in ArcGIS Pro)*

| Governorates | Total area (km$^2$) | Total inundated areas (km$^2$) | % of Inundated Area |
|---|---|---|---|
| Alexandria | 2,679 | 509 | 20% |
| Beheira | 9,826 | 2,320 | 23.6% |
| Dakahlia | 3,459 | 832 | 24% |
| Damietta | 910 | 498.5 | 54.7% |
| Gharbia | 1942 | 0.7 | 0.04% |
| Ismailia | 1,442 | 183.4 | 12.7% |
| Kafr El-Sheikh | 3,437 | 1,241.4 | 36.1% |
| Port Said | 1,303 | 1,036 | 79.5% |
| Sharqia | 4,911 | 302 | 6.1% |

***Table 5.*** *Statistics of vulnerable governorates due to SLR of 1 m. (Obtained from 1m scenario attribute table in ArcGIS Pro)*

With 2 m of SLR, the water will significantly extend more into the governorates, mainly Dakahlia, Damietta, Kafr El-Sheikh and Sharqia as shown in **Figure** 26, where the increment in the expected inundated areas from the previous scenario is 2553 km$^2$ and total inundated area is expected to be 9,476 km$^2$. Dakahlia and Sharqia will be impacted almost twice as much as in the first scenario. Gharbia will be the least affected in this scenario based on its inundated area percentage compared to its total area. **Table** 6 shows the total expected submerged areas in each governorate and their total areas.

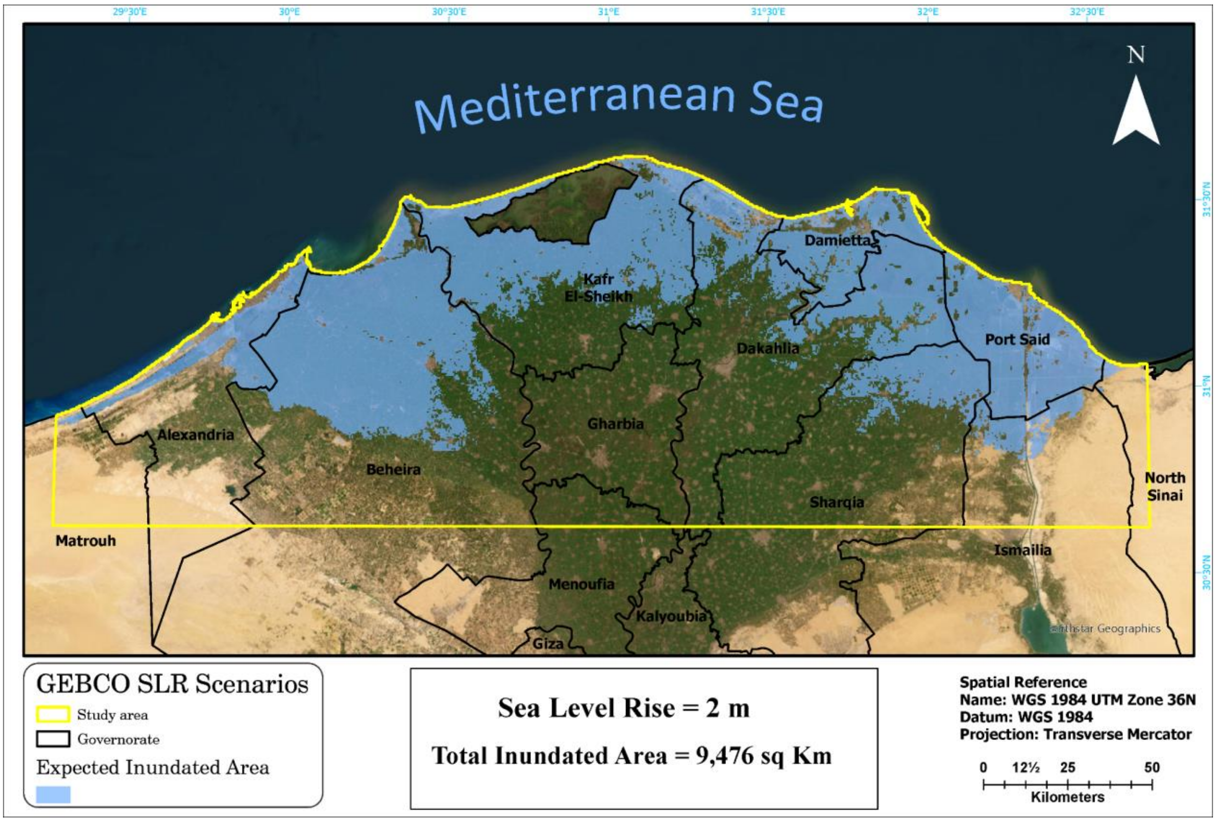


***Figure 26.*** *An inundation map of 2 m SLR with the affected areas. (Created by the author in ArcGIS Pro)*

| Governorates | Total area (km$^2$) | Total inundated areas (km$^2$) | % of Inundated Area |
|---|---|---|---|
| Alexandria | 2,679 | 536.4 | 20% |
| Beheira | 9,826 | 2,730 | 27.7% |
| Dakahlia | 3,459 | 1,440.8 | 41.7% |
| Damietta | 910 | 707.7 | 77.8% |
| Gharbia | 1942 | 3.9 | 0.2% |
| Ismailia | 1,442 | 261.5 | 18.1% |
| Kafr El-Sheikh | 3,437 | 1,995 | 58% |
| Port Said | 1,303 | 1,189.6 | 91.3% |

| | | | |
|---|---|---|---|
| Sharqia | 4,911 | 610.7 | 12.4% |

***Table 6.*** *Statistics of vulnerable governorates due to SLR of 2 m. (Obtained from 2 m scenario attribute table in ArcGIS Pro)*

On the other hand, with 3 and 4 m SLR, Beheira, Dakahlia, Kafr El-Sheikh will suffer drastically and they will lose more than half of their total areas (**Figure** 27) and **Table** 7 shows the statistics and consequences of increasing the water level to 3 m obviously where the increment difference in total inundated area compared on the previous scenario is 2087 km$^2$ with total inundated area of 11,563 km$^2$. Dakahlia and Damietta will be impacted by 20% and 10% more respectively compared to the 2 m scenario. In the 4 m scenario, the increment difference from the 3 m scenario is 1650 km$^2$, where Sharqia will suffer from more water creeping and lose around one fourth of its total area and Damietta will be almost submerged as shown in **Figure** 28 below visually with total expected inundated area in all governorates of 13,213 km$^2$ and **Table** 8 summarizes the total area lost by 4 m SLR for each governorate.

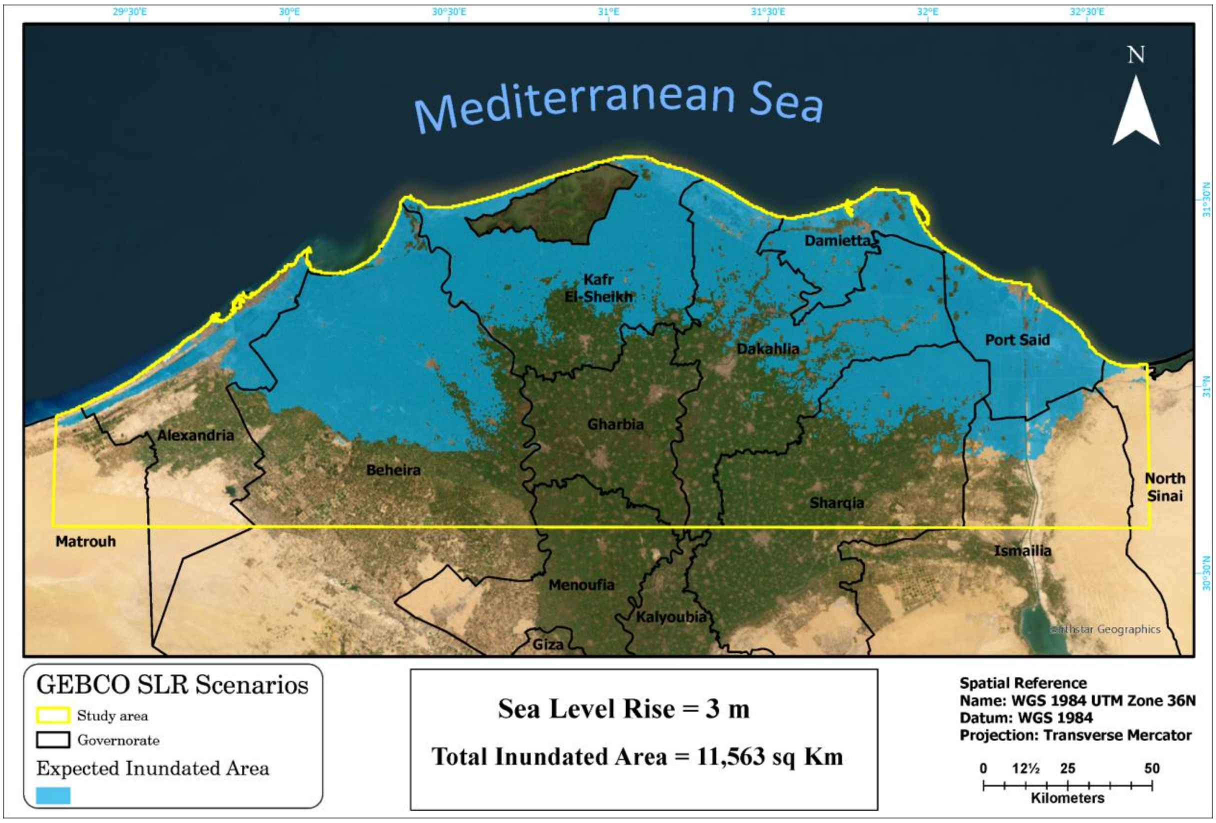


***Figure 27.*** *An inundation map of 3 m SLR with the affected areas. (Created by the author in ArcGIS Pro)*

| Governorates | Total area ($km^2$) | Total inundated areas ($km^2$) | % of Inundated Area |
|---|---|---|---|
| Alexandria | 2,679 | 560.3 | 20.9% |
| Beheira | 9,826 | 3,106.8 | 31.6% |
| Dakahlia | 3,459 | 2,211.2 | 63.9% |
| Damietta | 910 | 790.5 | 86.7% |
| Gharbia | 1942 | 25.7 | 1.3% |
| Ismailia | 1,442 | 325.4 | 22.6% |
| Kafr El-Sheikh | 3,437 | 2,400.5 | 69.8% |
| Port Said | 1,303 | 1,234.7 | 94.7% |
| Sharqia | 4,911 | 907.7 | 18.5% |

***Table 7.*** *Statistics of vulnerable governorates due to SLR of 3 m. (Obtained from 3m scenario attribute table in ArcGIS Pro)*

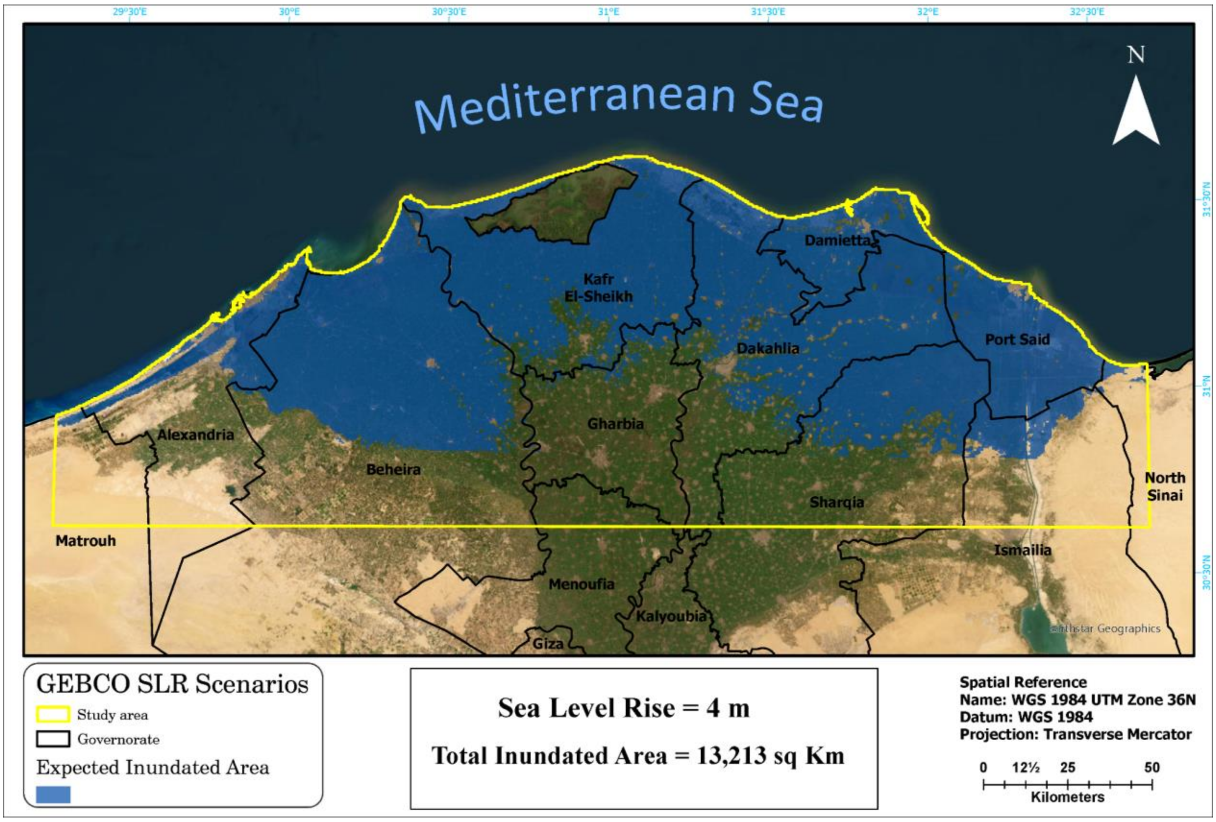


***Figure 28.*** *An inundation map of 4 m SLR with the affected areas. (Created by the author in ArcGIS Pro)*

| **Governorates** | **Total area (km$^2$)** | **Total inundated areas (km$^2$)** | **% of Inundated Area** |
|---|---|---|---|
| Alexandria | 2,679 | 582.4 | 21.7% |
| Beheira | 9,826 | 3,372.8 | 34.3% |
| Dakahlia | 3,459 | 2,756.8 | 79.7% |
| Damietta | 910 | 826.9 | 90.9% |
| Gharbia | 1942 | 121 | 6.2% |
| Ismailia | 1,442 | 354.4 | 24.6% |
| Kafr El-Sheikh | 3,437 | 2,789 | 81.1% |
| Port Said | 1,303 | 1,258.8 | 96.6% |

| | | | |
|---|---|---|---|
| Sharqia | 4,911 | 1151.6 | 23.4% |

***Table 8.*** *Statistics of vulnerable governorates due to SLR of 4 m. (Obtained from 4m scenario attribute table in ArcGIS Pro)*

### 4.2. SRTM SLR Scenarios

SRTM SLR geospatial analysis expected the total inundated area within the study area to be 41,770 km$^2$ as shown in the overview map below (**Figure** 29) when the water level reaches 4 meters with eliminating Matrouh, Menoufia, and North Sinai from the vector area calculation as they do not belong to the northern delta. This means the difference in total expected inundation area is about 177 km$^2$ only between GEBCO and SRTM. Below, we will also discuss the results of the four scenarios of SRTM and each one's impact on the governorates within the study area as it is important to see the contrast between both SRTM and GEBCO results based on the different spatial resolution, techniques and errors in terms of vertical accuracy.

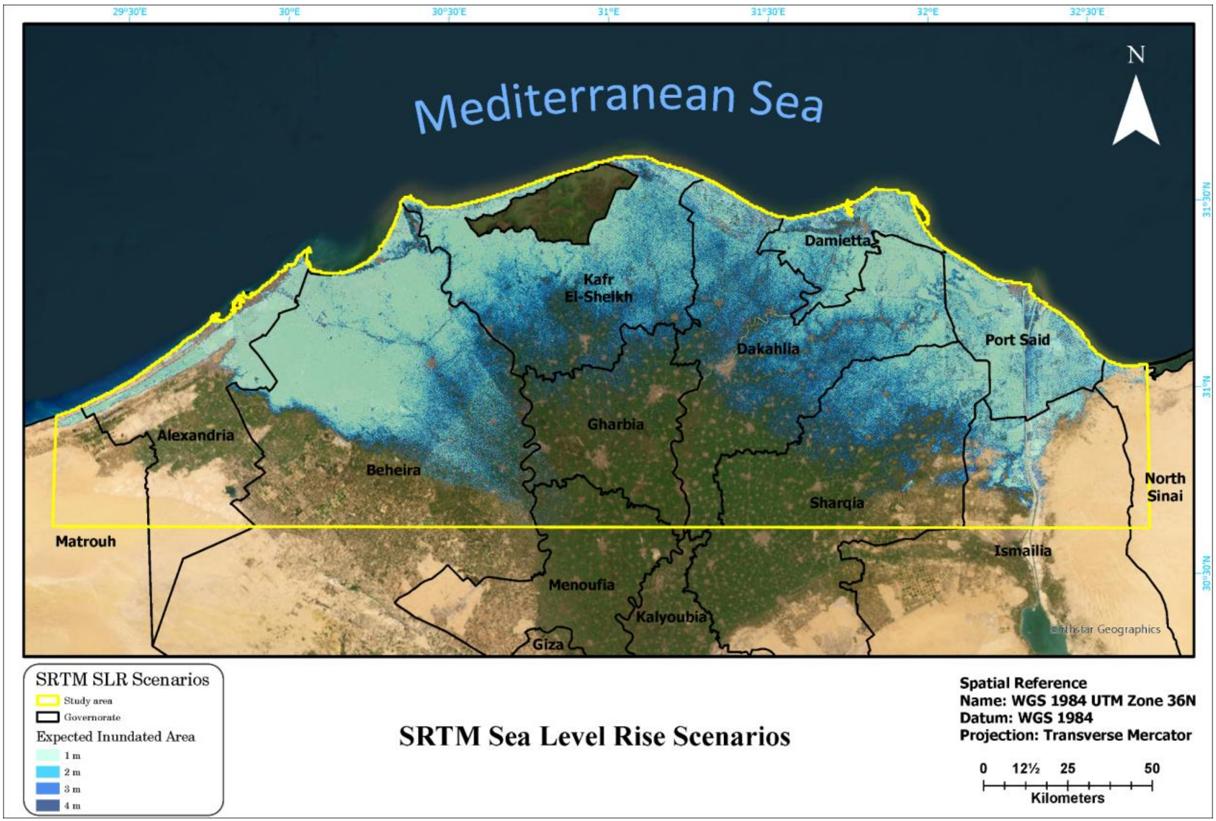


***Figure 29.*** *An overview map for the 4 SRTM SLR scenarios. (Created by the author in ArcGIS Pro)*

In case of 1 m SLR and same as in GEBCO's first scenario, northern coast part of Alexandria will be impacted, while Beheira, Dakahlia will lose around one fourth of their total area due to land submergence. Alexandria, Damietta, Kafr El-Sheikh and Port Said will be first inundated due to the above-mentioned reasons in GEBCO results (**Figure** 30) with a total inundated area of 7,277 $km^2$. The following table (**Table** 9) shows the total expected submerged areas in each governorate and their total area. Garbia is still the least impacted governorate so far based on the ratio of inundated area to the governorate's total area.

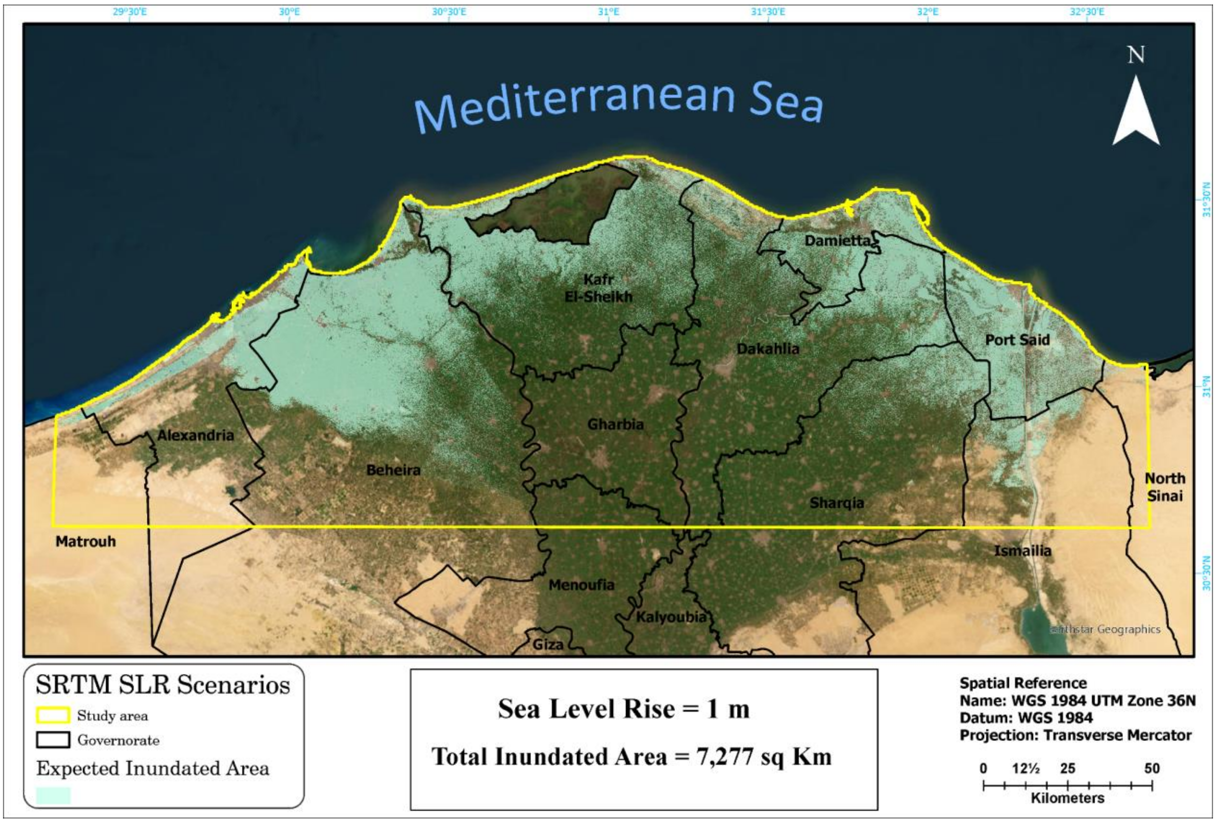


*Figure 30. An overview map for the 1 m SLR scenario with the affected areas. (Created by the author in ArcGIS Pro)*

| **Governorates** | **Total area ($km^2$)** | **Total inundated areas ($km^2$)** | **% of Inundated Area** |
|---|---|---|---|
| Alexandria | 2,679 | 514 | 19.2% |
| Beheira | 9,826 | 2,427 | 24.7% |
| Dakahlia | 3,459 | 993 | 28.7% |

| | | | |
|---|---|---|---|
| Damietta | 910 | 508 | 55.8% |
| Gharbia | 1942 | 16.5 | 0.8% |
| Ismailia | 1,442 | 247 | 17.1% |
| Kafr El-Sheikh | 3,437 | 1,309 | 38.1% |
| Port Said | 1,303 | 895 | 68.7% |
| Sharqia | 4,911 | 366.7 | 7.5% |

***Table 9.*** *Statistics of vulnerable governorates due to SLR of 1 m. (Obtained from 1m scenario attribute table in ArcGIS Pro)*

With 2 m of SLR, the water will significantly extend more into the governorates, mainly Dakahlia, Damietta, Kafr El-Sheikh and Sharqia as shown in **Figure** 31 with total inundated area of 9,519 km$^2$ and the increment in the expected inundated areas from the previous scenario is 2553 km$^2$. The water rise will impact Dakahlia by 18% and Damietta will lose three-quarters of its total area, while Port Said will lose 193 km$^2$ more of its total area. **Table** 10 shows the total expected submerged areas in each governorate and their total areas.

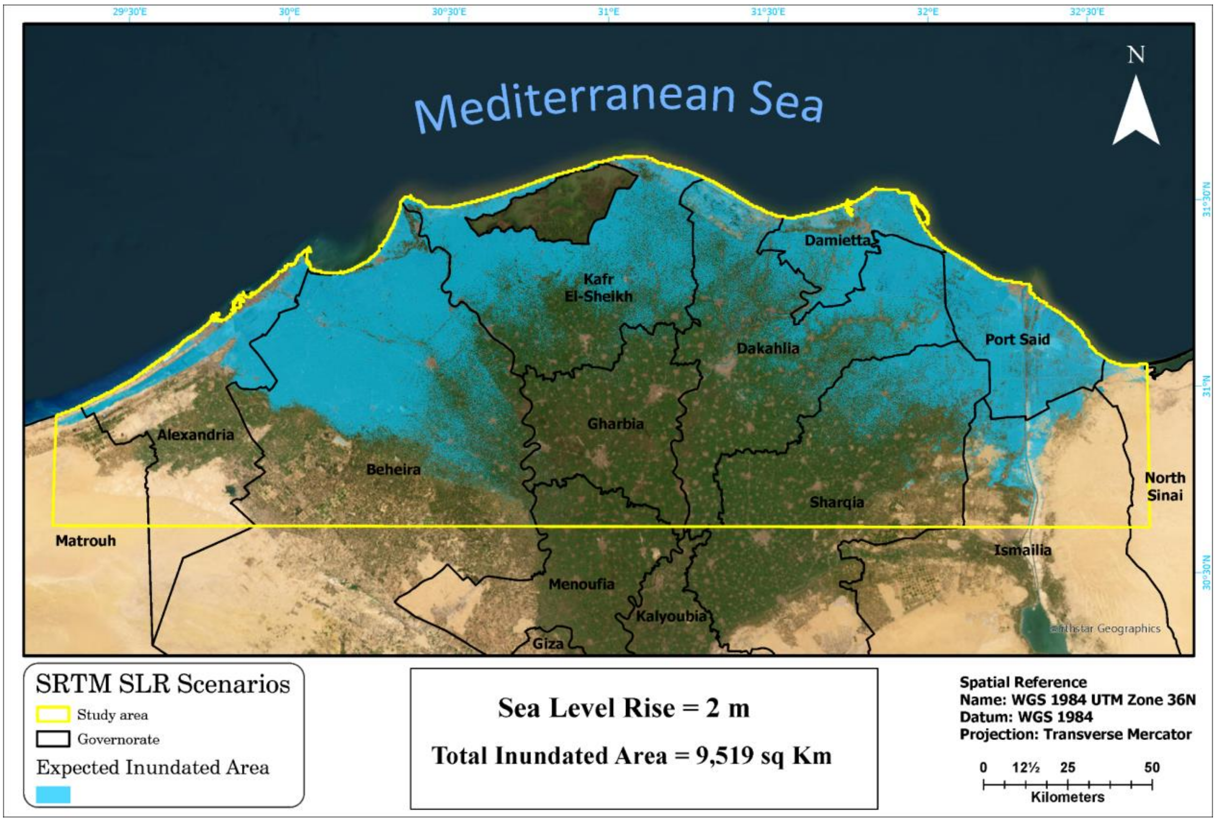


*Figure 31. An inundation map of 2 m SLR with the affected areas. (Created by the author in ArcGIS Pro)*

| Governorates | Total area (km$^2$) | Total inundated areas (km$^2$) | % of Inundated Area |
|---|---|---|---|
| Alexandria | 2,679 | 541.9 | 20.2% |
| Beheira | 9,826 | 2,811.5 | 28.6% |
| Dakahlia | 3,459 | 1,535.6 | 44.4% |
| Damietta | 910 | 661.4 | 72.7% |
| Gharbia | 1942 | 39.6 | 2% |
| Ismailia | 1,442 | 340.3 | 23.6% |
| Kafr El-Sheikh | 3,437 | 1,872.3 | 54.5% |
| Port Said | 1,303 | 1,088.5 | 83.5% |

| | | | |
|---|---|---|---|
| Sharqia | 4,911 | 628.4 | 12.8% |

***Table 10.*** *Statistics of vulnerable governorates due to SLR of 2 m. (Obtained from 2m scenario attribute table in ArcGIS Pro)*

In the third scenario, Dakahlia and Kafr El-Sheikh will suffer dramatically and will lose more than half of their total areas, while 90% of Port Said will be below water (**Figure** 32). **Table** 11 shows the statistics and consequences of increasing the water level to 3 m obviously where the total inundated area is expected to be 11,584 km$^2$ and the increase in inundated areas is 2065 km$^2$ compared to the second scenario. Sharqia will suffer from more water creeping and lose around one fourth of its area in the 4 m scenario and Damietta will be almost totally submerged with 90% inundated of its total area as shown in **Figure** 28 below visually. The total expected inundated area in all governorates is approximately 13,390 km$^2$ with an increase of inundated areas from the third scenario of 1806 km$^2$ and **Table** 12 summarizes the total area lost by 4 m SLR for each governorate.

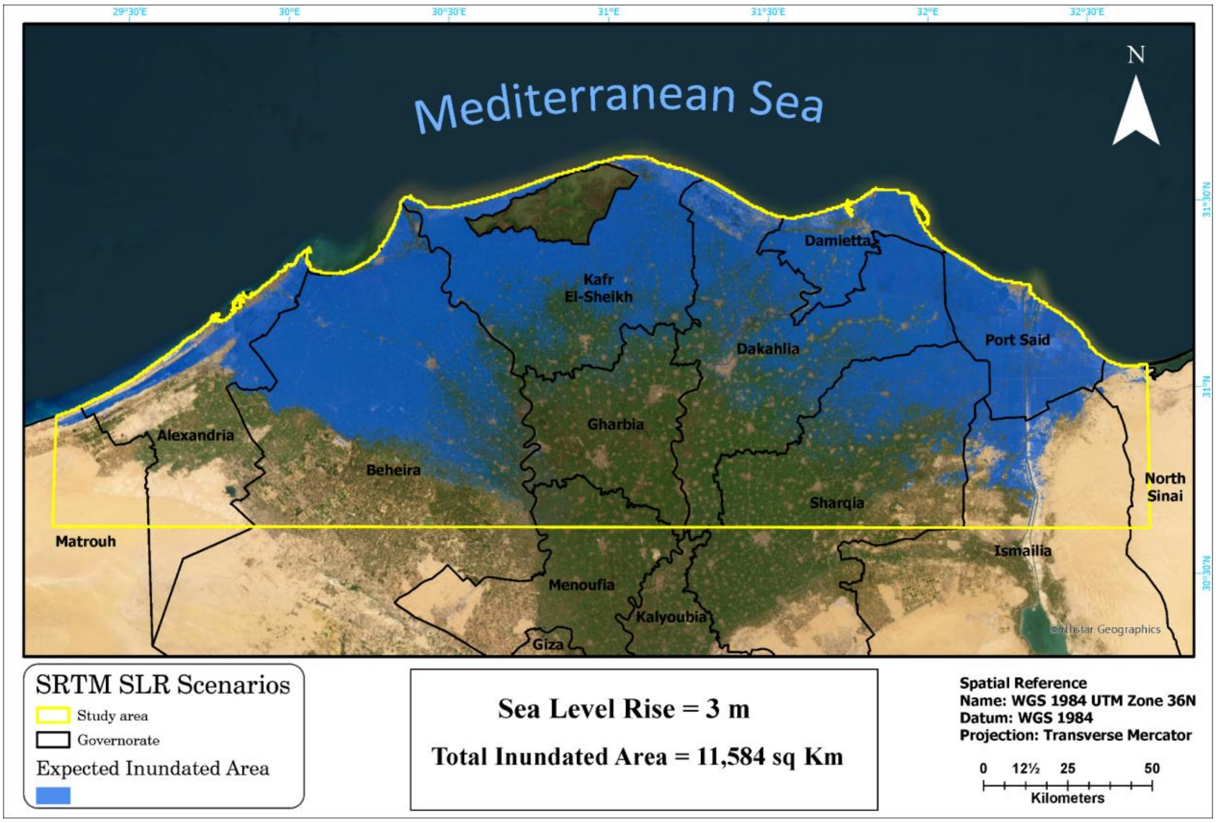


***Figure 32.*** *An inundation map of 3 m SLR with the affected areas. (Created by the author in ArcGIS Pro)*

| Governorates | Total area (km$^2$) | Total inundated areas (km$^2$) | % of Inundated Area |
|---|---|---|---|
| Alexandria | 2,679 | 566.4 | 21.1% |
| Beheira | 9,826 | 3,167.4 | 32.2% |
| Dakahlia | 3,459 | 2,117.3 | 61.2% |
| Damietta | 910 | 757 | 83.2% |
| Gharbia | 1942 | 107 | 5.5% |
| Ismailia | 1,442 | 423.3 | 29.4% |
| Kafr El-Sheikh | 3,437 | 2,339.5 | 68.1% |
| Port Said | 1,303 | 1,187.2 | 91.1% |
| Sharqia | 4,911 | 919.4 | 18.7% |

***Table 11.*** *Statistics of vulnerable governorates due to SLR of 3 m. (Obtained from 3m scenario attribute table in ArcGIS Pro)*

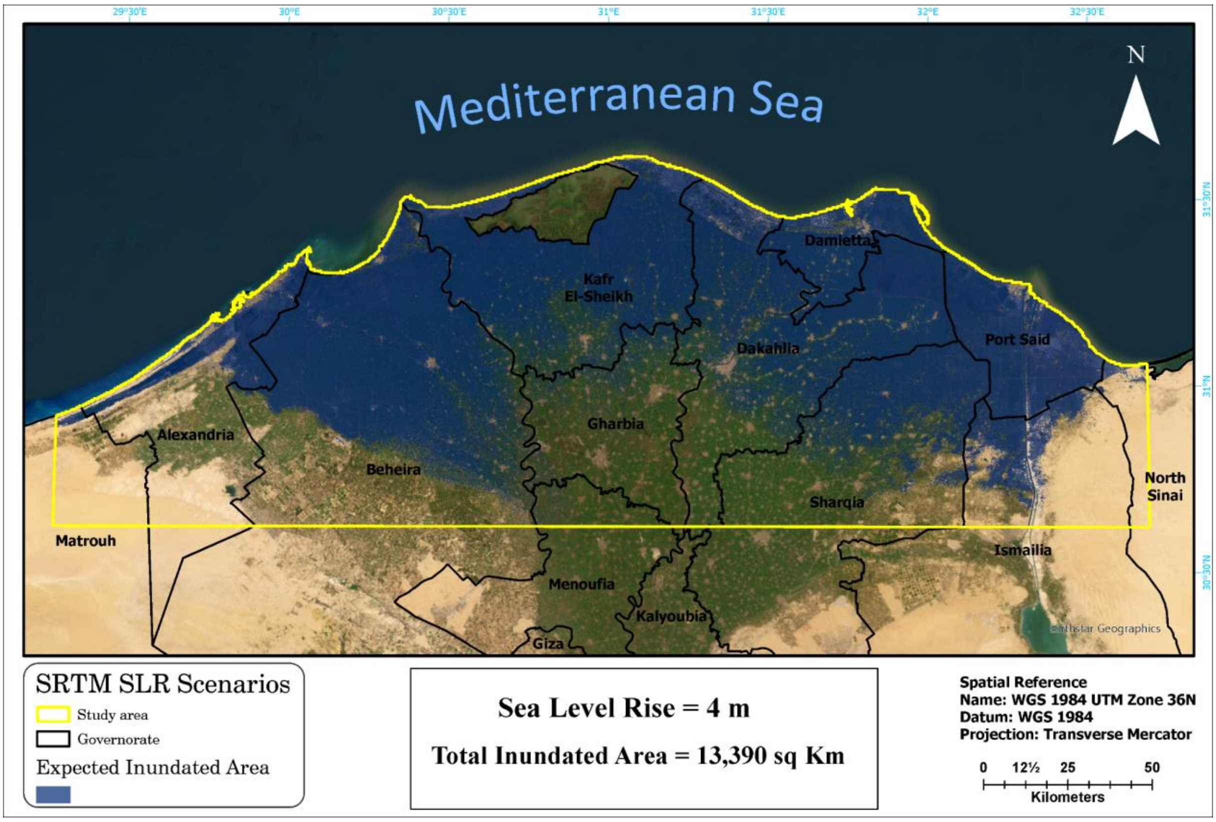


*Figure 33. An inundation map of 4 m SLR with the affected areas. (Created by the author in ArcGIS Pro)*

| Governorates | Total area (km²) | Total inundated areas (km²) | % of Inundated Area |
|---|---|---|---|
| Alexandria | 2,679 | 588.8 | 22% |
| Beheira | 9,826 | 3,473.4 | 35.3% |
| Dakahlia | 3,459 | 2,621.4 | 75.8% |
| Damietta | 910 | 809.9 | 89% |
| Gharbia | 1942 | 255.9 | 13.2% |
| Ismailia | 1,442 | 494.4 | 34.3% |
| Kafr El-Sheikh | 3,437 | 2,695.7 | 78.4% |

| | | | |
|---|---|---|---|
| Port Said | 1,303 | 1,234.4 | 94.7% |
| Sharqia | 4,911 | 1,216.5 | 24.8% |

***Table 12.*** *Statistics of vulnerable governorates due to SLR of 4 m. (Obtained from 4m scenario attribute table in ArcGIS Pro)*

### 4.3. SRTM and GEBCO Correlation

The geospatial DEM analysis indicates that in case of GEBCO four SLR scenarios, the percentages of total expected inundated areas compared to the total study area are 26%, 35.8%, 43.7% and 50% respectively. On the other hand, SRTM percentages in the same aspect were 27.5%, 36%, 43.8 and 50.6% subsequently. This evidently shows a noticeable correlation between SRTM and GEBCO results with high similarity in values where this is shown clearly in the chart below (**Figure** 34) where the difference between the four scenarios in both DEMs is a matter of few kilometers compared to total area of the study area and the small scale of the map.

In the first scenario, the difference is about 354 km$^2$, while it is 43 km$^2$ in the second scenario. In the third and fourth, it is about 21 km$^2$ and 177 km$^2$ respectively. It is also indicated that It is noticed that all SRTM total areas in all scenarios slightly exceed those of GEBCO and this is quite logical as SRTM has higher spatial resolution and smaller pixel size of 30 meters by 30 meters on the ground, so it can detect more detailed topography. This means in this case that SRTM with 30m spatial resolution could capture smaller-scale features such as hills, valleys, and small streams that may not be visible in a lower resolution DEM like in case of GEBCO.

However, it's important to take into consideration that increasing the resolution of a DEM may not always result in a more accurate representation of the terrain. Other factors such as the quality and processing of the data, the interpolation methods used, and the terrain characteristics can also affect the accuracy of the DEM. This is apparent when we have a look at governorates like Gharbia and Ismailia and check their inundated areas in both DEMs, we will find a a large contrast somehow in the results and this could be due to their different topography from the surrounding as they are higher in elevation that other governorates.

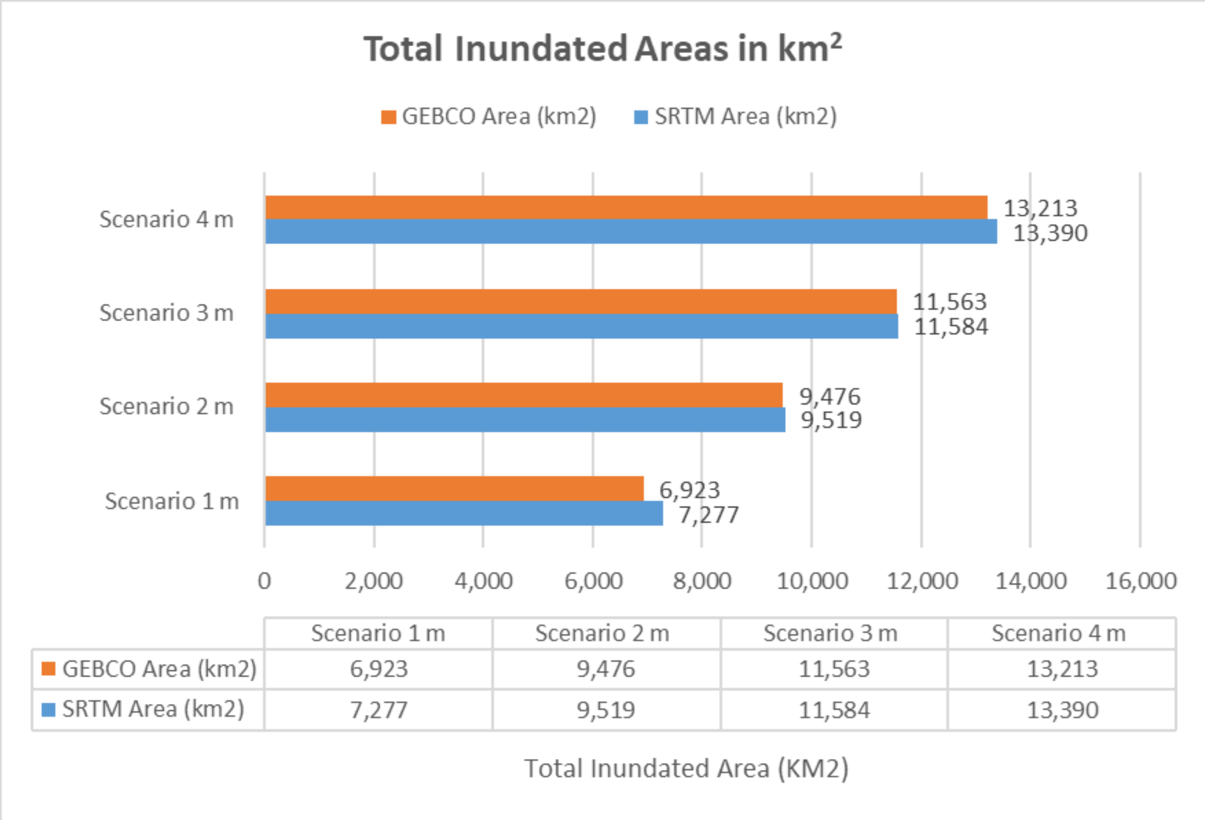


***Figure 34.*** *A clustered bar chart showing a comparison between total inundated areas estimated from SRTM and GEBCO for the 4 SLR scenarios. (Created by the author in MS Excel)*

# 5. CONCLUSIONS

In conclusion, SRTM and GEBCO datasets have substantiated their ability and capability as valuable remote sensing tools in detecting potential SLR in the future in the northern Nile Delta. By combining these DEMS, we could create simulations for different SLR scenarios and their potential impact on the region, such as flooding and coastal erosion. What fosters the applicability of SRTM and GIS techniques in monitoring the coastal flooding and SLR is that they were used already to identify the vulnerability of China's coastal region and low-lying areas at inundation risk (Yin et al., 2010). It is vital to emphasize on the applications of GIS and multi-temporal satellite imagery as elaborative techniques in assessing land degradation hazard indices and the current status of the Nile Delta which is prone to land degradation processes like water logging, salinization and urban sprawl (Shalaby et al., 2012). Excessive irrigation, interference with natural drainage systems, incorrect timing of heavy machinery use, and the lack of conservation measures are the primary factors that lead to human-induced land degradation in the area (El Baroudy, 2011).

However, it is a key factor in such analyses to keep in mind that DEMs are inevitably subjected to errors either during data acquisition or interpolation and if their errors are not eliminated, they can cause uncertainties to the results. Accuracy is usually a dependent factor of both vertical and horizontal resolutions. Regarding the Nile Delta, the vertical errors of SRTM range from ±3.1 meters to ±8.6 meters depending on the location and terrain, but still its accuracy is very good for the delta as one of the most commonly used GDEMs worldwide. Such errors can vary among different DEMS depending on the nature of the terrain, type of vegetation cover and presence of man-made structures. Therefore, local DEMs for the study area could be produced via using the country's precise topographic maps, remote sensing techniques like photogrammetry, LIDAR and GPS for applications that require higher accuracy such as engineering designs.

This research provides valuable insights for investigating the northern Nile Delta region using GEBCO freely accessed data in the public domain which can be used for informed decision making and policy development. As sea levels continue to rise globally, the use of SRTM and GEBCO datasets will remain essential tools for understanding and addressing the potential impacts of SLR in the Nile Delta region and other coastal areas around the world. Primary outcomes from both DEMs showed that 35% of the northern delta region could be totally submerged in case SLR reaches 2 meters by 2100 as many studies suggest. In the case of 4 meters, it will have a catastrophic effect as around half the delta will be inundated with about 13,000 $km^2$ of impacted total area. In all scenarios, Port Said, Damietta and Kafr El-Sheikh respectively will be amongst the first governorates to be affected by the SLR, not to mention that such a famous Mediterranean city like Alexandria will lose one-fourth of its total area due to inundation by SLR. Sentinel-2 land explorer classification also showed that croplands would be the most affected by the SLR impact, followed by built-up areas and bare soils.

In order to overcome and adapt to these challenges, some coastal management methods and risk assessments should be made and put into action. Successfully addressing water-related issues in the Nile Delta will require a significant level of awareness and understanding of the problems. One possible approach to improving this understanding is to promote education focused on sustainable resource management, including energy, soil, and water and enhancing the knowledge of the wider population and stakeholders in Egypt has a key role in improving the future of the Nile Delta (Reguero & Griggs, 2022).Virtual Reality technology could be introduced among the public to raise awareness and highlight key principles related to coastal risks and climate change as it can effectively facilitate new ways for visualizing SLR simulations in an interactive, immersive, and safe learning environment (Cazenave, 2019).

The continuous investigation of the Nile Delta geomorphology using high-resolution DEMs and multi-spectral satellite imagery is crucial to identify major threats to its sustainability and monitor the expansion of the extent of ponds and waterlogging that are replacing sabkhas and agricultural areas. Coastal defenses represented in building seawalls, barriers and dikes can reduce the impact of storm surges and SLR in coastal cities like Alexandria and Port Said. Beach nourishment via adding sediments to shorelines can help absorb the waves energy and reduce the erosion. Restoration of natural habitats and wetlands along the coast can also absorb storm surges and protect inland areas from submergence. Land use planning and implementing infrastructure adaptation via upgrading the bridges, roads and water supply systems could combat coastal flooding and SLR. Finally, the remote sensing community should work on integrating different remote sensing techniques and policies via conducting research, collaboration with policymakers, capacity building and developing tools and technologies such as early warning systems, risk maps and models to predict the impacts of SLR and coastal flooding.

# REFERENCES


Abdel-Aziz, T., Dawod, G., & Ebaid, H. (2020). DEMs and reliable sea level rise risk monitoring in Nile Delta, Egypt. *Discover Sustainability*, *1*(1). https://doi.org/10.1007/s43621-020-00006-7

Abou Samra, R. M., El-Gammal, M., Al-Mutairi, N., Alsahli, M. M., & Ibrahim, Mahmoud. S. (2021). GIS-based approach to estimate sea level rise impacts on Damietta coast, Egypt. *Arabian Journal of Geosciences*, *14*(6). https://doi.org/10.1007/s12517-021-06810-3

ASTER-GDEM (2011). ASTER global digital elevation model version 2 – summary of validation results. *NASA LPDAAC&JPL, pp., 1–27*.

Atkinson, P.M. & Tatnall, A.R. (1997). Introduction: remote sensing of the coastal zone. *International Journal of Remote Sensing*, *18*(11), 2341-2350. https://doi.org/10.1080/014311697218700

Cazenave, A. (2019). Satellite Altimetry. *Encyclopedia of Ocean Sciences*, *5*, 397–401. https://doi.org/10.1016/b978-0-12-409548-9.11624-0

Cazenave, A. & Llovel, W. (2010). Contemporary Sea Level Rise. *Annual Review of Marine Science*. 2 (1), 145–173. https://doi:10.1146/annurev-marine-120308-081105

Church, J. A., & White, N. J. (2006). A 20th century acceleration in global sea-level rise. *Geophysical Research Letters*, 33(1). https://doi.org/10.1029/2005gl024826

Church, J.A. & White, N.J. (2011). Sea-level rise from the late 19th to the early 21st century. *Surveys in Geophysics*, 32 (4–5), 585–602. https://doi:10.1007/s10712-011-9119-1

Daniell, J. (2010). The combination of soundings and remotely sensed bathymetry in the GEBCO grid. *Fifth Annual GEBCO Bathymetric Science Day.*

Dasgupta, S., Laplante, B., Murray, S., & Wheeler, D. (2009). Sea-level rise and storm surges: A comparative analysis of impacts in developing countries. *World Bank Policy Research Working Paper, (4901)*. https://doi.org/10.1596/1813-9450-4901

El Baroudy, A. A. (2011). Monitoring land degradation using remote sensing and GIS techniques in an area of the middle Nile Delta, Egypt. *CATENA*, *87*(2), 201–208. https://doi.org/10.1016/j.catena.2011.05.023

El Bastawesy, M., Cherif, O. H., & Sultan, M. (2016). The geomorphological evidences of subsidence in the Nile Delta: Analysis of high resolution topographic DEM and multi-temporal satellite images. *Journal of African Earth Sciences*, *136*, 252–261. https://doi.org/10.1016/j.jafrearsci.2016.10.013

El-Nahry, A. H., & Doluschitz, R. (2010). Climate change and its impacts on the coastal zone of the Nile Delta, Egypt. *Environmental Earth Sciences,59*(7), 1497–1506.

El-Quilish, M., El-Ashquer, M., Dawod, G., & Fiky, G. E. (2018). Development and Accuracy Assessment of High-Resolution Digital Elevation Model Using GIS Approaches for the Nile Delta Region, Egypt. *American Journal of Geographic Information System*, *7*(4), 107–117. https://doi.org/10.5923/j.ajgis.20180704.02

El-Quilish, M., El-Ashquer, M., Dawod, G., & Fiky, G. E. (2022). Development of an Inundation Model for the Northern Coastal Zone of the Nile Delta Region, Egypt Using High-Resolution DEM. *Arabian Journal for Science and Engineering*, *48*(1), 601–614. https://doi.org/10.1007/s13369-022-07013-y

El-Raey, M. (1997). Vulnerability assessment of the coastal zone of the Nile delta of Egypt, to the impacts of sea level rise. *Ocean & Coastal Management*, *37*(1), 29–40. https://doi.org/10.1016/s0964-5691(97)00056-2

El-Raey, M., Frihy, O., Nasr, S. M., & Dewidar, Kh. (1999). Vulnerability Assessment of Sea Level Rise Over Port Said Governorate, Egypt. *Environmental Monitoring and Assessment*, *56*(2), 113–128. https://doi.org/10.1023/a:1005946819600

Eldeberky, Y. (2011). Coastal adaptation to sea level rise along the Nile delta, Egypt. *WIT Transactions on Ecology and the Environment*, *149*, 41–52. https://doi.org/10.2495/cp110041

Eldeberky, Y., & Hünicke, B. (2015). Vulnerability of the Nile Delta to recent and future climate change. E-proceedings of the 36th IAHR World Congress.

Elsaka, B., Radwan, A. M., & Rashwan, M. (2020). Evaluation of Nile Delta-Mediterranean Sea Conjunction Using GPS, Satellite-Based Gravity and Altimetry Datasets. *Journal of Geoscience and Environment Protection*, *08*(02), 33–46. https://doi.org/10.4236/gep.2020.82003

Elshinnawy, I. A., & Almaliki, A. H. (2021). Vulnerability Assessment for Sea Level Rise Impacts on Coastal Systems of Gamasa Ras El Bar Area, Nile Delta, Egypt. *Sustainability*, *13*(7), 3624. https://doi.org/10.3390/su13073624

ESA. (2021). *ERS' Contribution to Altimetry [Governmental]*. https://earth.esa.int/eogateway/news/ers-contribution-to-altimetry

FitzGerald, D. M., Fenster, M. S., Argow, B. A., & Buynevich, I. V. (2008). Coastal impacts due to sea-level rise. *Annual Review of Earth and Planetary Sciences*, *36*, 601-647. https://doi.org/10.1146/annurev.earth.35.031306.140139

Fraser, C. S. and Ravanbakhsh, M. (2011). Performance of DEM generation technologies in coastal environments. *The 7th International Symposium on Digital Earth*, *40–49*.

Frihy, O. E. (2003). The Nile delta-Alexandria coast: vulnerability to sea-level rise, consequences and adaptation. *Mitigation and Adaptation Strategies for Global Change*, *8*(2), 115–138. https://doi.org/10.1023/a:1026015824714

Gorokhovich, Y., & Voustianiouk, A. (2006). Accuracy assessment of the processed SRTM-based elevation data by CGIAR using field data from USA and Thailand and its relation to the terrain characteristics. *Remote Sensing of Environment*, *104*(4), 409–415. https://doi.org/10.1016/j.rse.2006.05.012

Haars, C., Winkelaar, B., Lönsjö, E., & Mogos, B. (2016). *The uncertain future of the Nile Delta*. https://doi.org/10.13140/RG.2.1.1837.0963

Hasan, E., Khan, S. I., & Hong, Y. (2015). Investigation of potential sea level rise impact on the Nile Delta, Egypt using digital elevation models. *Environmental Monitoring and Assessment*, *187*(10), 649. https://doi.org/10.1007/s10661-015-4868-9

Hassaan, M. A., & Abdrabo, M. A. (2012). Vulnerability of the Nile Delta coastal areas to inundation by sea level rise. *Environmental Monitoring and Assessment*, *185*(8), 6607–6616. https://doi.org/10.1007/s10661-012-3050-x

Heinz Center. (2000). Coastal elevations and sea-level rise: National and regional implications. The H. John Heinz III Center for Science, Economics and the Environment, Washington, DC.

Hereher, M. E. (2010). Vulnerability of the Nile Delta to sea level rise: an assessment using remote sensing. *Geomatics, Natural Hazards and Risk*, *1*(4), 315–321. https://doi.org/10.1080/19475705.2010.516912

Hussien, A. A., Mohamed, M. G. M., Yousef, P. H. A., Hagag, M. R., & Seoud, T. A. E. (2021). Sensitivity of Enhanced SRTM for Sea-Level Rise Variation on Egyptian Coasts. *Civil Engineering and Architecture*, *9*(3), 958–968. https://doi.org/10.13189/cea.2021.090337

Intergovernmental Panel of Climate Change (IPCC). (2001). Climate change 2001: Impacts, adaptations, and vulnerability. *Contribution of Working Group II to the third assessment report of the Intergovernmental Panel on Climate Change*. Cambridge, UK, and New York: Cambridge University Press.

Karlsson, J. M., & Arnberg, W. (2011). Quality analysis of SRTM and HYDRO1K: a case study of flood inundation in Mozambique. *International Journal of Remote Sensing*, *32*(1), 267–285. https://doi.org/10.1080/01431160903464112

Lindsey, R. (2020). Climate change: Global sea level. https://www.climate.gov/news-features/understanding-climate/climate-change-global-sea-level, Accessed 8 Apr 2023.

Luijendijk, A., Hagenaars, G., Ranasinghe, R., Baart, F., Donchyts, G., & Aarninkhof, S. (2018). The state of the world's beaches. *Scientific Reports*, *8*(1), 6641. https://doi.org/10.1038/s41598-018-24630-6

Marriner, N., Flaux, C., Morhange, C., & Kaniewski, D. (2012). Nile Delta's sinking past: Quantifiable links with Holocene compaction and climate-driven changes in sediment supply?. *Geology*, *40*(12), 1083–1086.

Mimura, N. (2013). Sea-level rise caused by climate change and its implications for society. *Proceedings of the Japan Academy, Series B, 89*(7), 281–301. https://doi.org/10.2183/pjab.89.281

Musa, Z. N., Popescu, I., & Mynett, A. (2015). A review of applications of satellite SAR, optical, altimetry and DEM data for surface water modelling, mapping and parameter estimation. *Hydrology and Earth System Sciences (HESS), 12,* 4857–4878. https://doi.org/10.5194/hessd-12-4857-2015

NASA JPL (2013). NASA Shuttle Radar Topography Mission Global 1 arc second [Data set]. NASA EOSDIS Land Processes DAAC. Accessed 2023-05-03 from https://doi.org/10.5067/MEaSUREs/SRTM/SRTMGL1.003

Parris, A., Bromirski, P., Burkett, V., Cayan, D., Culver, M., Hall, J., Horton, R., Knuuti, K., Moss, R., Obeysekera, J., et al. (2012). Global Sea Level Rise Scenarios for the United States National Climate Assessment. *NOAA Tech Memo OAR CPO-1, NOAA, Silver Spring, MD*.

Refaat, M. M., & Eldeberky, Y. (2016). Assessment of Coastal Inundation due to Sea-Level Rise along the Mediterranean Coast of Egypt. *Marine Geodesy*, *39*(3-4), 290–304. https://doi.org/10.1080/01490419.2016.1189471

Reguero, B. G., & Griggs, G. (2022). Editorial: Adaptation to Coastal Climate Change and Sea-Level Rise. Water, *14*(7), 996. https://doi.org/10.3390/w14070996

Sefelnasr, A., & Sherif, M. (2013). Impacts of Seawater Rise on Seawater Intrusion in the Nile Delta Aquifer, Egypt. *Groundwater*, *52*(2), 264–276. https://doi.org/10.1111/gwat.12058

Shalaby, A., Ali, R. R., & Gad, A. (2012). Land Degradation Monitoring in the Nile Delta of Egypt, using Remote Sensing and GIS. *International Journal of Basic and Applied Sciences*, *1*(4), 292–303. http://www.crdeepjournal.org/wp-content/uploads/2012/10/Vol-143-IJBAS1.pdf

Spalding, M.D., Ruffo, S., Lacambra, C., Meliane, I., Hale, L.Z., & Shepard, C.C. (2014). The role of ecosystems in coastal protection: adapting to climate change and coastal hazards. *Ocean & Coastal Management, 90,* 50-57. https://doi.org/10.1016/j.ocecoaman.2013.07.001

SRTM-DEM, 2006. Shuttle radar topography mission DTED level 1 (3-arc second) documentation. *NASA/LPDAAC and USGS/EROS*, 1–8.

Stanley, D. J. (1990). Recent subsidence and northeast tilting of the Nile delta, Egypt. *Marine Geology*, *94*(1-2), 147–154.

Vitousek, S., Buscombe, D., Vos, K., Barnard, P. L., Ritchie, A. C., & Warrick, J. A. (2023). The future of coastal monitoring through satellite remote sensing. *Cambridge Prisms: Coastal Futures*, *1*, E10. Cambridge Core. https://doi.org/10.1017/cft.2022.4

Yin, J., Xu, S., Wang, J., Zhong, H., Hu, Y., Yin, Z., Wang, K., & Zhang, X. (2010). Vulnerability assessment of combined impacts of sea level rise and coastal flooding for China's coastal region using remote sensing and GIS. *The 18th International Conference on Geoinformatics*, 1–4. https://doi.org/10.1109/GEOINFORMATICS.2010.5567562

# DECLARATION

I, undersigned *Ahmed Hussien Gaber Mohamed Hamido* (NEPTUN CODE: *VSVR2A*), declare that the present master's thesis is my original intellectual product in full and that I have not submitted any part or the whole of this work to any other institution. Permissions related to the use of copyrighted sources in this work are attached.

I agree to the publication of the accepted master's thesis in pdf form on the website of the Department of Cartography and Geoinformatics.

Budapest, *15, 05, 2023*

*(signature of the student)*